Reports of the Department of Geodetic Science

Report No. 162

AN INVESTIGATION INTO SOME PROBLEMS OF LUNAR ORBITER PHOTOGRAPHY SYSTEM

by

Dr. Peter James Morgan

Prepared for

National Aeronautics and Space Administration
Office of Scientific and Technical Information (Code US)
Washington, D.C. 20546

Grant No. NGR 36-008-125
OSURF Project No. 2810

Interim Report

The Ohio State University
Research Foundation
Columbus, Ohio 43212

August, 1971

Reports of the Department of Geodetic Science
Report No. 162

Title: AN INVESTIGATION INTO
SOME PROBLEMS OF
LUNAR ORBITER PHOTOGRAPHY SYSTEM

Sponsor: National Aeronautics and Space Administration
Office of Scientific and Technical Information
(Code US)
Washington, D. C. 20546

Interim Report
NASA Grant No. NGR 36-008-125
OSURF Project No. 2810

Prepared by: Dr. Peter James Morgan
Graduate Research Associate

Submitted by: Department of Geodetic Science
The Ohio State University

Dr. Sanjib K. Ghosh
Associate Professor
Research Supervisor

Date: August, 1971

FOREWORD

This project is under the supervision and guidance of Dr. Sanjib K. Ghosh, Associate Professor in the Department of Geodetic Science. The project with NASA Grant No. NGR 36-008-125, which is a part of the research program at NASA's Manned Spacecraft Center, Houston, Texas was administered by NASA, Washington, D.C. with Mr. Joseph T. Davis as the Grant s Officer; Mr. John P. Simpson as the NASA Negotiator. Mr. Paul E. Norman, and on his death, later, Mr. Robert Hill acted as the Technical Monitor.

This report covers research performed by Dr. Peter James Morgan, Mr. G. B. Das and Mr. Aldwyn Philip, Research Associates; Miss V. Filippakopoulou, Mr. John Oswald, Research Assistants; Mr. Alan Palo, Technical Assistant; Mrs. G. Swisher, Mrs. Patricia Roa, Research Aids, and Dr. S. K. Ghosh, Research Superviser.

ACKNOWLEDGMENT

The research work documented in this report has been supported by the National Aeronautics and Space Administration through a research grant (NGR 36-008-125). This grant provided financial support for which the author is most grateful.

The author wishes to thank Dr. S. K. Ghosh, his adviser and Project Supervisor, for the initial direction and subsequent support and encouragement throughout the period of the project. Special mention must also be made of the assistance given by Drs. D. Merchant, R. Rapp and U. Uotila of the Department of Geodetic Science and Mr. John Snowden of the Instruction and Research Computer Center who maintained an open-door policy to the author.

Support for this work in the form of computer facilities was generously made available by Dr. R. Reeves of the IRCC, while operational support was rendered by Mrs. Martha Finch and Mr. Ronald Vershinski and their respective staffs.

Mrs. G. Swisher provided essential secretarial support during the period of research, while Mr. Alan Palo assisted with drafting.

The author is also indebted to Dr. Colin Bull, Chairman of the Department of Geology, for providing the initial opportunity to study at The Ohio State University and for his constant advice and assistance during these difficult but enjoyable years.

In conclusion, my thanks must go to my wife for her patience and understanding during this period of study, and especially for her practical assistance in typing this report.

TABLE OF CONTENTS

TABLE OF CONTENTS
(Continued)

LIST OF TABLES

LIST OF FIGURES

* * * * * * * * * * *

LIST OF PLATES

LIST OF SYMBOLS

In the notation associated with this report, a number of principles have been adhered to.

(a) The symbols A, B, C, D, E are usually matrix quantities of dimensions (n x m) or (n x n).

(b) The symbols i, j, k, l, m, n are usually constants.

(c) The symbols U, V, W, X, Y, Z are usually vector quantities of dimensions (n x 1).

(d) Lower case symbols are single quantities, while upper case symbols usually represent arrays.

(e) Where possible, the normally-accepted nomenclature is used to represent the quantity.

(f) Where a symbol has more than one meaning, the meaning assigned to a particular section is indicated.

****

f	the calibrated focal length of the camera
x_p, y_p	x and y coordinates of an image point
x_o, y_o	x and y coordinates of the principal point
Δx, Δy	image displacements

v_x, v_y — x and y image velocities

$\dot{x}_p$, $\dot{y}_p$ — x and y instantaneous image velocities

Δt — the exposure epoch

κ, ϕ, ω — the attitude of the camera axis. The order of the rotations is tertiary, secondary, primary, respectively

$\dot{\kappa}$, $\dot{\phi}$, $\dot{\omega}$ — the rates of change of camera axis attitude

X_o — a vector of coordinates representing the photostation

$$X_o = \begin{bmatrix} X \\ Y \\ Z \end{bmatrix}_o$$

X_p — a vector of object space coordinates

$$X_p = \begin{bmatrix} X \\ Y \\ Z \end{bmatrix}_p$$

V — a vector of velocity components of the photostation (used in Chapter 2)

$$V = \begin{bmatrix} V_x \\ V_y \\ V_z \end{bmatrix}$$

M — the general three-dimensional rotation matrix

$M = R_\kappa R_\phi R_\omega$ (used in Chapter 2, Appendices A, F)

M_i — the ith row of the general rotation matrix M: i = 1, 2, 3

N — the augmented rotation matrix $N = R_{\chi} R_{\dot{\kappa}\Delta t} R_{\phi} R_{\dot{\phi}\Delta t} R_{\omega} R_{\dot{\omega}\Delta t}$ (Used in Chapter 2, Appendices A, F)

N_i — the ith row of the augmented rotation matrix N: i = 1, 2, 3

$\dot{N}_i$ — the derivative of the ith row of N with respect to Δt

$\|X\|$ — a vector norm

$\|A\|$ — a matrix norm

M — the Turing M number (used in Chapter 3)

N — the Turing N number (used in Chapter 3)

H — the Hadamard Condition number (used in Chapter 3)

P — the Todd P number (used in Chapter 3)

P — the weight matrix $P = \sum_{L_b}^{-1}$ (used in Chapter 4)

X_{oo} — the approximate values of the parameters

X_a — the adjusted values of the parameters

L_a — the adjusted values of the observations

L_b — the observed values of the observations

L_o	approximate values of the observations computed through the model
V	a vector of residuals $V = L_b - L_a$ (used in Chapter 4)
ϵ	a discrepancy vector $\epsilon = L_b - L_o$
λ	a vector of Lagrange multipliers
A	partial differential matrix of function with respect to observed quantities.
B	partial differential matrix of function with respect to parameters
E_B	partial differential matrix of function with respect to elements of exterior orientation
S_B	partial differential matrix of function with respect to survey parameters
Δ	the correction vector to be applied to the approximate values to obtain the adjusted values $X_a = X_{oo} + \Delta$
E_Δ	the correction vector for the elements of exterior orientation
S_Δ	the correction vector for the survey parameters
$\sum$	the variance-covariance matrix

$\tilde{\sigma}_{ij}$ the ij element of the variance-covariance matrix

$NX + U = 0$ { the general symbolic form of the reduced matrix system

1. INTRODUCTION

1.0 Scope and Objectives

Two principal types of camera are currently available to photogrammetrists. The first type is, from a historical viewpoint, the ideal camera for a mapping photogrammetrist, since it usually combines low objective distortion characteristics with a high degree of stability. That is, its laboratory calibration can be assumed to apply under a wide range of conditions for an extended time period. The classical cameras of this type are the Wild RC and the Zeiss RMK series of aerial cameras.

The second type of camera is comparatively new to photogrammetry. It is characterized by high image quality and information content, but not so stable geometry. The class is typified by the panoramic and focal plane shutter cameras manufactured by Itek and Hycon.

Unfortunately, current technology in the design and manufacture of large-format camera systems is such that the two types of camera are almost mutually exclusive. Consequently, while the first group of cameras has been used almost exclusively for mapping purposes, the second group has been used almost exclusively for photointerpretation tasks. Recently, this distinction has begun to break down dramatically, with cameras from the second or non-metric group

being used more and more in small-scale metric tasks where the amount of information content is paramount.

One of the first breaks in class distinction and use occurred in the mid-sixties, when NASA chose a non-metric photo subsystem to accomplish the metric task of mapping the Apollo zone of the moon. Unfortunately, at that time the geometric fidelity and stability of non-metric cameras were incompletely understood. This resulted in data mis-matches and discrepancies for the lunar triangulation.

The general trend of previous work on non-metric cameras had been directed towards a complete understanding of the optical quality of the resulting image and those factors which affected it. There was now a need to also understand the geometric fidelity of the image. This study therefore seeks to provide meaningful answers to the following general problems which arise when non-metric cameras are used for metric work.

(a) What is the effect of image motion and image motion compensation on the location of the principal point?

(b) Is it possible to determine the corrections to the calibrated values of the coordinates (defining the location of the principal point or the fiducial centre) in order to correct for the image motion compensation?

(c) What is the effect of the focal plane shutter on the distortion and interior geometry (interior orientation parameters)?

(d) Can a lack of calibration information be overcome by dynamic calibration procedures incorporated in the photographic mission?

In view of the relevance of these studies to the particular needs of NASA, the Lunar Orbiter Photographic Subsystem will be used to typify a non-metric system.

Chapter 2 details a new mathematical model which takes into consideration image motion and movement of the camera during the exposure interval. The model offers a rigorous relationship between the object space and the image space by incorporating into the well-known collinearity conditions velocity terms for the exposure station. The model is considered general since it is possible to apply simplifying assumptions to obtain the presently-accepted explanation for image motion. Unfortunately, these gains in generality have been accompanied by increased complexity of the model and consequently possible computational instability problems.

Chapter 3 is devoted to some of the problems faced in the solution of large systems of equations. The two principal problems treated are computational stability and the economic solution of such equations by non-iterative methods. The segment on computational stability introduces the concept of matrix and vector norms. The concept is then developed through perturbation theory into an acceptable method for gauging the stability of a particular solution. The final half of the chapter investigates a number of possible alternative methods for the solution of large matrix systems.

Chapter 4 is concerned with numerical testing of the model proposed in Chapter 2. The tests are all made with simulated lunar data for which true values of all parameters are known. The chapter has three main subdivisions. The first details the method of

generating the simulated data. The second section discusses the single photo resection tests, while the third section discusses the general intersection problem. Particular attention is given in all tests to the problem of computational stability and to the control of this problem by the choice of the correct weight matrix of the observed quantities.

Finally Chapter 5 reviews and summarizes the work of Chapters 2, 3 and 4 in terms of the four above-mentioned problems.

1.1 Historical Review

The Lunar Orbiter program was conceived primarily for the acquisition of high-quality photographic data from those portions of the lunar surface under consideration for the Apollo program.

Prior to the launching of Lunar Orbiter I, man's photographic coverage of the moon consisted of earth-based photography by telescopes whose maximum resolution on the lunar surface was approximately 20 metres[1]. A detailed discussion on the limiting factors for this type of coverage is given in the ACIC report "Department of Defense 1966 Selenodetic Control Data"[1]. A very small amount of additional coverage at greater resolution, but with very high geometric distortion, was obtained from the Ranger missions. The reduction of this material was accomplished almost exclusively by photometric techniques[2].

Table 1 summarizes the Lunar Orbiter missions[3].

Table 1

Summary of Lunar Orbiter Missions

Lunar Orbiter	Orbit Period (hr)	Inclination to Equatorial Axis (deg)	Perilune Altitude (km)	Apolune Altitude (km)	Date of Photography	Quality of Photography	
						Medium Resolution	High Resolution
I	3.5	12 and 21	60	1850	August 18-29, 1966	Acceptable	Unusable IMC failed
II	3.5	12 and 21	60	1850	November 18-25, 1966	Good	Good
III	3.5	12 and 21	60	1850	February 15-23, 1967	Excellent	Excellent
IV	12	85	2700	6100	May 11-26, 1967	Mediocre to poor	Excellent
V*	8.4	85	200	6000	August 8-18, 1967	Excellent	Excellent
	8.3	85	100	6000		Excellent	Excellent
	3.2	85	100	1500		Excellent	Excellent

* The three values represent the three conditions under which photography was obtained

The success of Lunar Orbiters II and III in acquiring the prime Apollo landing site data, coupled with the successful Surveyor flights to the moon, caused a reevaluation of the Lunar Orbiter IV mission. Thus the task of extrapolating the point information of the Surveyor missions and the forthcoming Apollo missions was to be done with the aid of a full lunar coverage obtained by Lunar Orbiter IV.

1.2 The Lunar Orbiter Photographic Subsystem

The Lunar Orbiter Photographic Subsystem has been completely described by the Eastman Kodak Company[4], subcontractors to The Boeing Company for the Lunar Orbiter program. In addition, specific parts of the Lunar Orbiter Photographic Subsystem have been described and discussed in the scientific literature, e.g. Konecny[5], Kosofsky[6], and Norman[7]. Despite this wealth of information, it is appropriate to discuss here certain aspects of the system so that a clear understanding of the research discussed in this report is obtained.

The Lunar Orbiter Photographic Subsystem incorporated two optical systems which imaged on the same 70 mm film. The 80 mm focal length system, often referred to as the medium resolution system, used a between-the-lens shutter system and a 55 x 65 mm format. Image Motion Compensation (IMC) was possible in a single direction, corresponding to the direction of movement of the focal plane shutter in the 610 mm system. The magnitude of this compensation was determined by a V/H sensor using an unimaged segment of the high

resolution imagery. A mechanical reduction linkage between the platen of the 610 mm system, where the determined IMC was applied, and the platen of the 80 mm system provided IMC for the 80 mm system.

The interior orientation for the 80 mm system was determined by laboratory calibration techniques. The subcontractor for this work was the Fairchild Camera Company[8]. The calibration included radial and tangential distortion components at discrete points along each of the principal diagonals.

The 610 mm system, often referred to as the high resolution system, used a focal plane shutter which traversed the short dimension of the 55 x 219 mm format. As previously indicated, IMC could be applied only in the direction of motion of shutter. This resulted in the IMC device remaining unactivated for the Lunar Orbiter IV mission. Figure 1 illustrates the different configurations controlling the applicability of IMC.

The camera was only partially calibrated by Brown[9] due to operational restrictions. Thus all missions were flown with non-recoverable photographic systems in which both the decentering distortion of the photographic system and one of the coordinates of the principal point (y) were unknown.

All photography derived from the Lunar Orbiter spacecraft was processed on board the spacecraft by the Kodak Bimat process. The resulting image was electronically scanned and transmitted back to earth where it was reassembled. Unfortunately, the framelets suffered distortion which can only be minimized. The reduction and

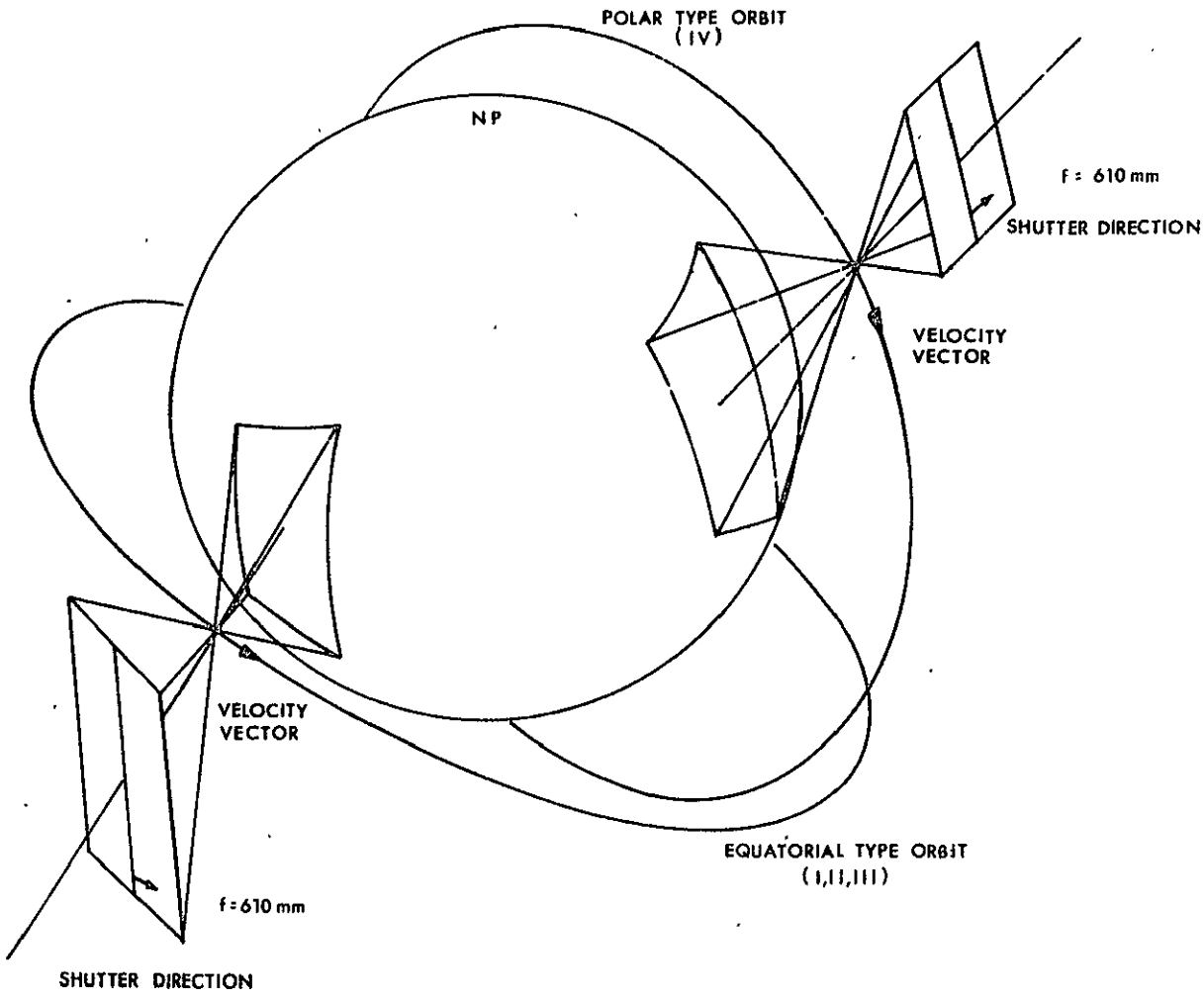

FIGURE 1

DIAGRAM ILLUSTRATING THE ORBIT AND CAMERA ORIENTATION FOR MISSIONS I, II, III, AND IV

elimination of this type of distortion is a comparatively new problem in photogrammetry. Fortunately, a considerable effort is being made into understanding the causes, effects and elimination of this distortion. Interested readers are referred to the work of Wong[10].

Throughout this report, it is assumed that the error sources of this problem have been identified and therefore need not be considered.

2. IMAGE MOTION AND IMAGE MOTION COMPENSATION

2.0 Introduction

In the late fifties and early sixties, considerable technical advances were made in all classes and types of cameras. In particular a new type of camera, the reconnaissance camera, became firmly established. Since this camera stresses image quality over geometric fidelity, it is the natural complement of the survey camera which is geometrically stable but has relatively poor resolution. The initial need for high image-quality systems was generated by military surveillance. Today, however, civilian needs for such a system are also very great, especially if the possibilities of extraterrestrial photogrammetry and photointerpretation are to be maximized.

Unfortunately, the operational requirements which necessitate these high-resolution systems are not favorable to geometric photogrammetry, since the photostation cannot be considered as a unique point in space. This movement of the photostation causes the image to blur. The amount of blur represents the magnitude of image motion present during the exposure interval. This degradation of the image cannot be tolerated and hence Image Motion Compensation (IMC) has been incorporated into these systems. The first detailed study of the degrading effects of image motion on

a photographic image was reported in 1955 by Wolfe and Lamberts[11]

There are three main methods of accomplishing IMC. They are as follows:

(a) Movement of the platen-film assembly.

(b) Movement of the lens cone.

(c) Use of the focal plane shutter.

Often method (c) is combined with (a) or (b). Application of method (a) or (b) destroys the interior geometry of the camera as currently conceived, while method (c) represents an infinite number of photographs joined side by side from a continuously changing photostation. For these reasons, systems which employ IMC have not been favored by mapping photogrammetrists. An exception is the recently developed Fairchild KC-6A camera.

The initial researchers in this new field of image degradation due to motion (Wolfe and Lamberts[11], Trott[12], Rosenau[13]) were all primarily concerned with the quality of the image without regard to its geometric position. In 1963, Kawachi and Weinflash[14] derived expressions for image velocities as functions of image position, focal length and rotational velocities. The expressions were not general but provided an acceptable method of determining expected blur distances and hence degradation under certain given conditions. The work of Kawachi and Weinflash was subsequently published in Photogrammetric Engineering[15].

This article was preceded by a discussion of image motion resulting from translations only[16]. Subsequent to these two papers by Kawachi, there are no published investigations on the

problems of image motion. Unfortunately, this could be due to the following statement by Kawachi[15].

> ... An analytical derivation involving matrices was also considered since a rotation matrix transforms the coordinates of a point in one system to its coordinates in a rotated coordinate system. It appears logical, therefore, that matrices can be applied to obtain the image velocity, since the aircraft motions under consideration are rotational. However the matrix approach is not appropriate for two reasons: (1) matrices do not describe the actual movement of the image point (unless additional translational terms are introduced to account for the changes in the radius vector), because the image remains in the film plane and hence its motion is not equivalent to holding the image point fixed and rotating the coordinate system; and (2) the matrix approach is not simpler than the geometrical approach but actually involves more equations. Multiplications of the matrices would show this ...

A similar statement is to be found in the Fairchild Technical Memo Note referenced above.

Unfortunately, the engineers and scientists in charge of the Lunar Orbiter Missions chose a photographic system of the reconnaissance type for their mapping program. This decision was, in part, influenced by the resolution of such systems. However, it was to lead to a number of awkward problems. In particular, the problem of image motion and its compensation has severely limited the accuracy of the subsequent triangulations, since Kawachi's formulae do not interconnect the object and image spaces. These formulae are therefore not applicable for direct incorporation into the mathematical relationships between the two spaces.

After failing to adequately incorporate Kawachi's formulae into the mathematical model, it became apparent that a new approach was needed. It was thus decided to investigate the feasibility of

using the collinearity conditions, since these conditions describe the existing relationships between object and image space systems.

2.1 The Collinearity Condition Approach

The well-known collinearity condition is, briefly speaking, a functional relationship between points in the object space and the image space systems. A complete derivation of this relationship may be found in most texts on photogrammetry, e.g. Manual of Photogrammetry[17]. The relationship is often written in a form that is pertinent to the user's particular purpose. In this work, it was desirable to express the collinearity condition in the following form:

$$x_p - x_o = -f\left[M_1(X_p - X_o) \,/\, M_3(X_p - X_o)\right]$$
$$y_p - y_o = -f\left[M_2(X_p - X_o) \,/\, M_3(X_p - X_o)\right] \qquad (2.1)$$

That is, given the position and attitude of the camera, it is possible to compute for every object space point a corresponding image space point. There is no restriction as to what type of surface the object space field must satisfy.

2.11 Augmentation of the Collinearity Condition Relationship

Consider a moving photographic platform over a stationary object space field. Photograph 1 is taken at $X_o = X_o^1$ and yields image points x_p^1, y_p^1. Photograph 2 is taken at $X_o = X_o^2$ and yields image points x_p^2, y_p^2 for the same object space field X_p. The platform is assumed to move with a three-dimensional velocity V. It

is known from the basic laws of mechanics that $X_o^2 - X_o^1 = V \cdot \Delta t$, hence alternative expressions for x_p^2, y_p^2 are:

$$x_p^2 - x_o = -f\left[M_1(X_p - X_o^1 - V\Delta t) \,/\, M_3(X_p - X_o^1 - V\Delta t)\right]$$
$$y_p^2 - y_o = -f\left[M_2(X_p - X_o^1 - V\Delta t) \,/\, M_3(X_p - X_o^1 - V\Delta t)\right] \qquad (2.2)$$

The displacement of the image due to the movement between the two photostations may be computed as:

$$\Delta x = x_p^2 - x_p^1 = -f\left[M_1(X_p - X_o^1 - V\Delta t) \,/\, M_3(X_p - X_o^1 - V\Delta t)\right] - f\left[M_1(X_p - X_o^1) \,/\, M_3(X_p - X_o^1)\right]$$
$$\Delta y = y_p^2 - y_p^1 = -f\left[M_2(X_p - X_o^1 - V\Delta t) \,/\, M_3(X_p - X_o^1 - V\Delta t)\right] - f\left[M_2(X_p - X_o^1) \,/\, M_3(X_p - X_o^1)\right] \qquad (2.3)$$

Expansion and simplification of equation set (2.3) yields the following image displacements:

$$\Delta x = -f\,\frac{M_1\left[(X_p - X_o^1)M_3V - VM_3(X_p - X_o^1)\right]\Delta t}{M_3(X_p - X_o^1 - V\Delta t)\cdot M_3(X_p - X_o^1)}$$
$$\Delta y = -f\,\frac{M_2\left[(X_p - X_o^1)M_3V - VM_3(X_p - X_o^1)\right]\Delta t}{M_3(X_p - X_o^1 - V\Delta t)\cdot M_3(X_p - X_o^1)} \qquad (2.4)$$

Logically, image velocities due to translation of the photostation may be readily computed from the above expressions as

$$v_x = \frac{\Delta x}{\Delta t} \quad \text{and} \quad v_y = \frac{\Delta y}{\Delta t}$$

Similarly, it is possible to describe image changes due to changes in the attitude rates. It is recognized that

$$M = \begin{bmatrix} M_1 \\ M_2 \\ M_3 \end{bmatrix} = R_\kappa R_\phi R_\omega$$

Then, by virtue of the double angle formulae, it is possible to define

$$N = \begin{bmatrix} N_1 \\ N_2 \\ N_3 \end{bmatrix} = R_\kappa R_{\dot\kappa \cdot \Delta t} R_\phi R_{\dot\phi \cdot \Delta t} R_\omega R_{\dot\omega \cdot \Delta t}$$

Thus

$$N = R_{(\kappa + \dot\kappa \cdot \Delta t)} R_{(\phi + \dot\phi \cdot \Delta t)} R_{(\omega + \dot\omega \cdot \Delta t)}$$

where $\dot\kappa$ = rate of change of κ,

$\dot\phi$ = rate of change of ϕ, (See Appendix A)

and $\dot\omega$ = rate of change of ω.

Hence the general expressions for image space coordinates of a moving system at any time with respect to a defined epoch, $\Delta t = 0$ are:

$$\begin{aligned} x_p - x_o &= -f\left[N_1(X_p - X_o - V\Delta t) / N_3(X_p - X_o - V\Delta t)\right] \\ y_p - y_o &= -f\left[N_2(X_p - X_o - V\Delta t) / N_3(X_p - X_o - V\Delta t)\right] \end{aligned} \qquad (2.5)$$

In the above derivations, the rate functions have been assumed to be constant. However, this is a mathematical simplicity that can quickly be removed.

By definition, image velocity is $\dot x_p$ and $\dot y_p$ and hence differentiation of equation set (2.5) with respect to Δt yields the

following instantaneous image velocity expressions:

$$\dot{x}_p = -f\Big\{\Big[\dot{N}_1(X_p - X_o - V\Delta t) - N_1 V\Big]\cdot\Big[N_3(X_p - X_o - V\Delta t)\Big] - \Big[\dot{N}_3(X_p - X_o - V\Delta t) - N_3 V\Big]\cdot\Big[N_1(X_p - X_o - V\Delta t)\Big]\Big\}\cdot \Big[N_3(X_p - X_o - V\Delta t)\Big]^{-2}$$

$$\dot{y}_p = -f\Big\{\Big[\dot{N}_2(X_p - X_o - V\Delta t) - N_2 V\Big]\cdot\Big[N_3(X_p - X_o - V\Delta t)\Big] - \Big[\dot{N}_3(X_p - X_o - V\Delta t) - N_3 V\Big]\cdot\Big[N_2(X_p - X_o - V\Delta t)\Big]\Big\}\cdot \Big[N_3(X_p - X_o - V\Delta t)\Big]^{-2} \qquad (2.6)$$

where $\dot{N}_1 = \frac{dN_1}{d\Delta t}$, similarly for $\dot{N}_2$ and $\dot{N}_3$. (See Appendix A.)

Equation sets (2.5) and (2.6) are completely general and without restriction as to the initial orientation of the camera, the form of the object space, the time interval, Δt, over which computations are to be considered, or the magnitudes of the impressed rates. They may therefore be called "general" equations for the context of this study.

2.2 Comparison of the General Theory with Kawachi's Theory

It can be demonstrated numerically that under the same initial conditions similar values are obtained for the general theory and the pertinent formulae of Kawachi. However, a stronger case exists by virtue of the fact that it is possible to decompose equation set (2.6) into the forms given by Kawachi[15, 16]. This decomposition is demonstrated in Appendix B using specific

examples.

Thus, equation set (2.6) appears to be the general equation set for all forms and causes of image motion for frame-type cameras where the collinearity condition is the same as that initially assumed. The equation set (2.6) must be modified for panoramic photography, since equation set (2.1) is not applicable.

2.3 Some Implications of the General Theory

Equation sets (2.5) and (2.6) were derived without any assumptions as to camera type (other than those satisfying the basic equation set (2.1)) They are therefore applicable to between-the-lens shutter systems as well as focal plane shutter systems. In the former case, every image point moves during the time interval, Δt, that the shutter is open, whereas in the case of focal plane shutters each segment may be viewed as an independent exposure during which image blur may or may not occur. If the exposure of each strip is sufficiently short then no detectable image motion will be seen, although image distortion will be present. This distortion is fully explained by equation set (2.5)

2.31 The 80 mm System of Lunar Orbiter

The 80 mm system of Lunar Orbiter was a between-the-lens shutter system with one component of IMC driven from a V/H sensor designed to detect net forward velocity. Thus the film was advanced or retarded at the required rate to minimize image blur. Variations in this rate have little meaning since it is a between-

the-lens system. The net effect of IMC is to produce a stationary photostation and consequently no photogrammetric reduction problems are envisaged except those resulting from data transmission or from a lack of stability of the interior orientation elements.

2.32 The 610 mm System of Lunar Orbiter

The 610 mm system for Lunar Orbiter had a focal plane shutter adjustable for 3 exposure times (1/25, 1/50, and 1/100 sec.). IMC could only be applied in the direction of flight and was computed from an on-board V/H sensor. Thus, the application of IMC is not constant unless the V/H ratio is constant. The photograph therefore suffers from two distortions:

(a) That due to the focal plane shutter and predicted by equation set (2.5) if Δt of each segment from some epoch is known.

(b) That due to forward motion IMC. This could be removed from the image coordinates on a summation basis by multiplying the applied IMC rate by Δt, the time lapse from epoch to moment of consideration.

In the case of Lunar Orbiters I, II, III and V, both (a) and (b) type distortions are present, while for Lunar Orbiter IV only type (a) distortions are present. (Actually, some blur is also present due to lack of IMC. This is because the direction of appliable IMC was not in the direction of the net forward motion.) That is, for focal plane cameras in which IMC was not used, equation set (2.5) fully describes the relationships between the object and image spaces. The important parameter is Δt, which

represents the segment exposure time along the x-axis with respect to some defined epoch, preferably defined as $\Delta t = 0$ when $x_p = 0$. A suitable method of obtaining Δt is available from the following data:

(a) Exposure interval - controls blind slit width.

(b) Blind velocity and direction.

However as the blind slit width approaches the dimensions of the format, then the focal plane shutter system becomes equivalent to the between-the-lens shutter system.

2.4 Some Experimental Results for Image Motion

Using equation set (2.6) a number of computer runs were made simulating the 80 mm and 610 mm systems of the Lunar Orbiter program. The results of some of these simulations have been collated into Plates I and II; Plate I considers translational velocities and their effects while Plate II considers the rotational velocities. Both studies are made using the assumption that the photographic system was initially vertical. Each plate has four major sub-sections dealing with each system at two different flying elevations. The sub-sections are composed of four separate graphs which indicate the expected magnitudes of the x- and y-directed image motion velocities for four important positions of the format. These positions are as follows, top to bottom and left to right, within each sub-section:

(a) $x_p = 0$, $y_p = \max$.

(b) $x_p = \max$, $y_p = \max$, an extreme corner.

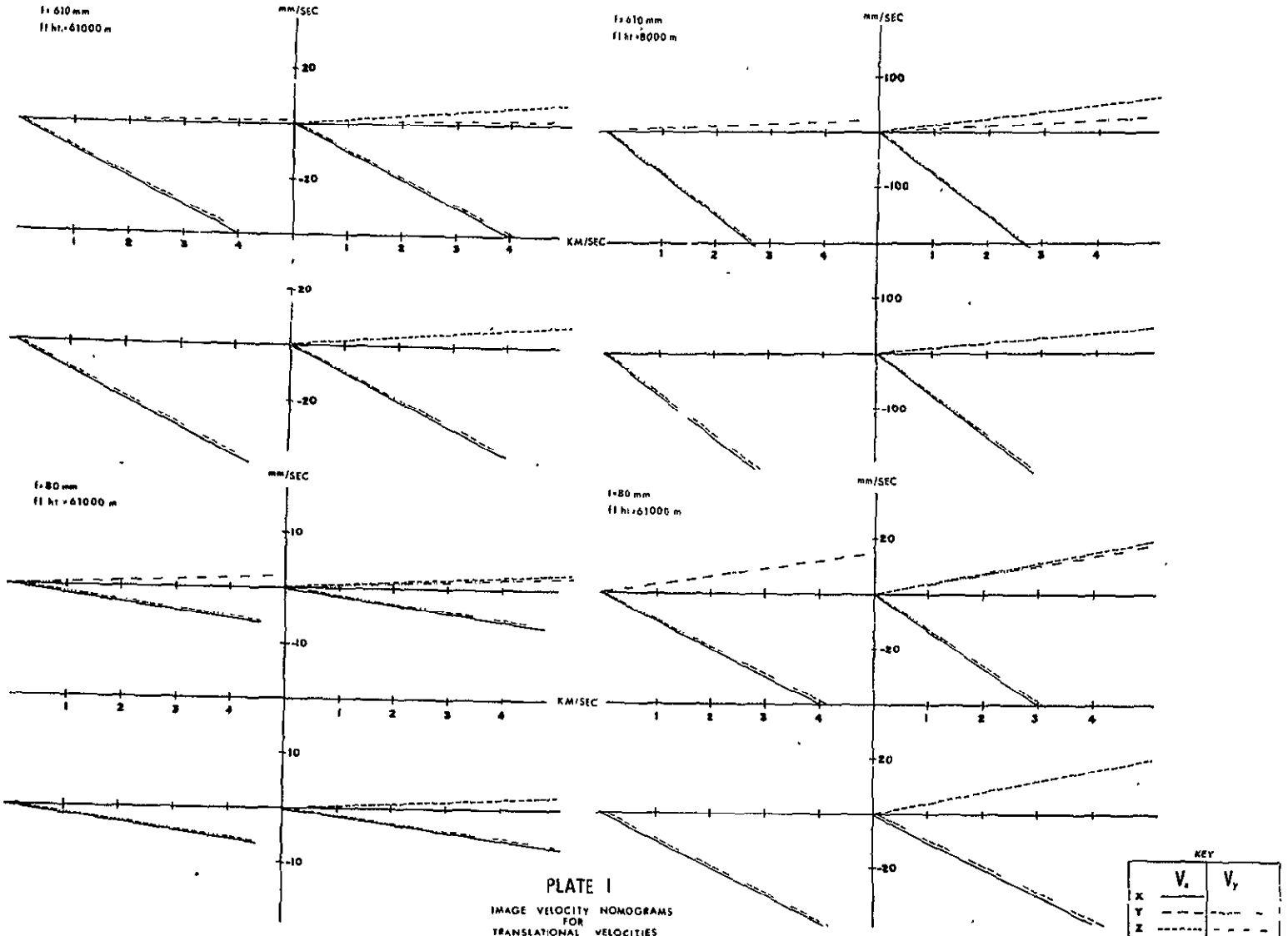

PLATE I

IMAGE VELOCITY NOMOGRAMS FOR TRANSLATIONAL VELOCITIES

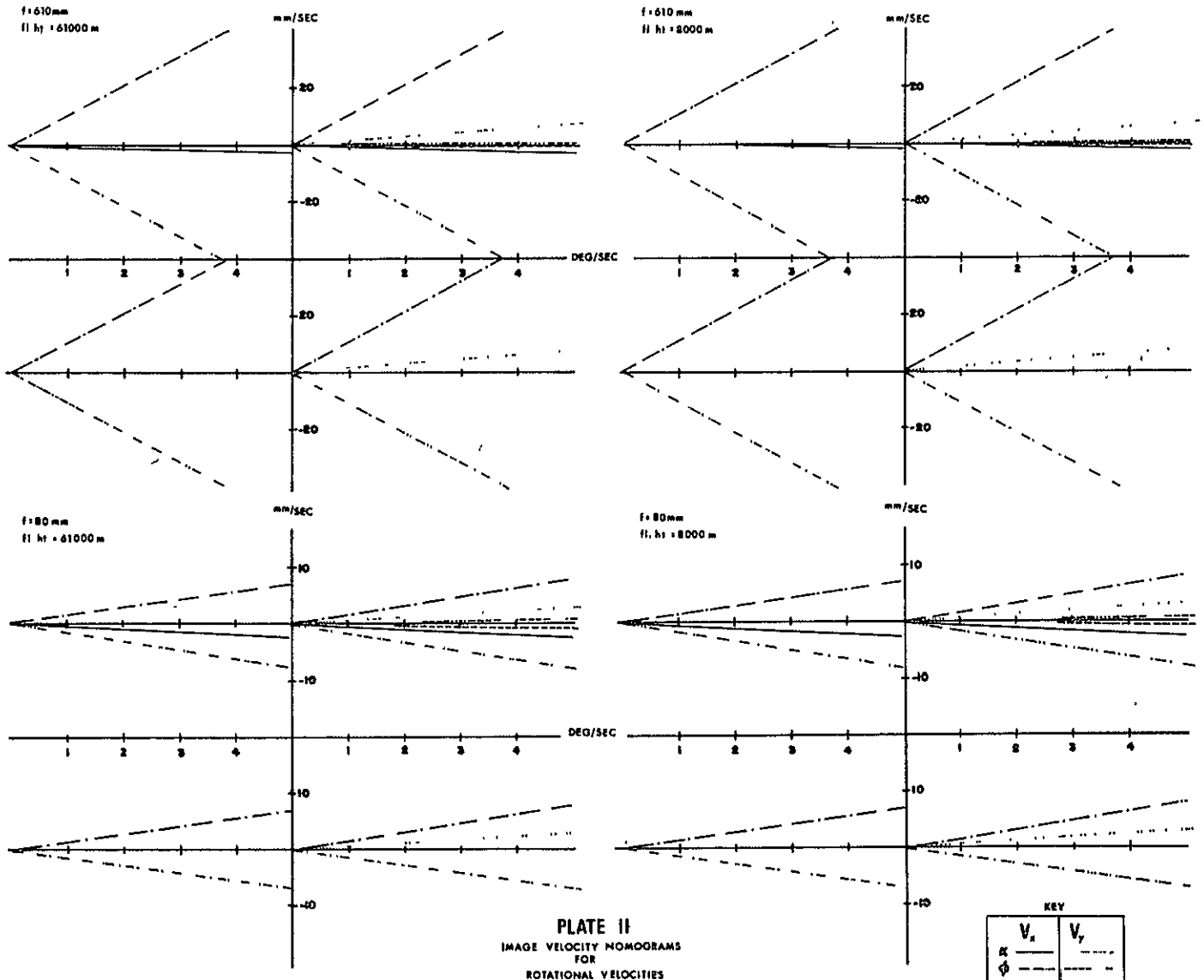

PLATE II

IMAGE VELOCITY NOMOGRAMS
FOR
ROTATIONAL VELOCITIES

(c) $x_p = 0$, $y_p = 0$, center of format.

(d) $x_p = \max$, $y_p = 0$.

It is apparent from Plates I and II that not all image velocities are plotted. It may be assumed that those not plotted are zero or of such small magnitude that they can be considered as zero.

An analysis of Plates I and II readily shows that for rotational velocities it is the focal length of the camera system that is important, regardless of the scale of the photograph. In the case of translational velocities, it is the scale of the photograph that is important in determining the magnitude of the expected image veolcity. Unfortunately, long focal lengths are normally used to increase photographic scale and hence both effects are present in the Lunar Orbiter systems. It is also most unlikely that the image motion effects can be made to cancel each other.

2.5 Conclusions

Equation set (2.5) is therefore an adequate representation of the processes controlling the functioning of both the 80 mm and 610 mm systems of Lunar Orbiter IV. Should photography from the 610 mm system of the other missions be considered for triangulation, then equation set (2.6) must also be considered. This would be quite complex, unless some simplifying assumptions could be made.

It is suspected from previous experiences that the velocity terms are heavily correlated with their respective photostation parameters. If this correlation is of such a nature as to make

the system "singular", then it will be necessary to apply conditions on the velocity parameters in order to obtain acceptable solutions for the unknown parameters of equation set (2.5).

Equation set (2.6) fully describes the nature and magnitude of any expected image motion due to translation and rotation of the camera during the exposure interval. It therefore represents two functional relationships which describe the nature of image velocity in terms of the elements of interior and exterior orientation.

3. MATRIX THEORY

3.0 Introduction

Methods for solving systems of normal equations date from the Gauss-Legendre era of the early nineteenth century, although the solution of small sets of simultaneous equations was already well-developed at that time. Thus, before the days of even the most modest digital computer, algorithms for either inverting or solving small- to medium-sized systems were well-known. Since the advent of the modern digital computer, the size of such systems has continued to increase, offering a unique field of endeavour for some scientists.

Geodetic scientists, in their quest to accurately describe the earth and her near neighbours, have consistently been in the forefront as users and developers of such systems. However, such use and development has seldom been tempered with an adequate numerical analysis of the problem.

In photogrammetry, the problem of inverting and/or solving a large system of equations resulting from a simultaneous, multi-station triangulation is already formidable. The proposed augmentation of the collinearity conditions places an even greater burden on the algorithms and computing machinery in present use. Furthermore, it has long been recognised that it is not normally

possible to simultaneously isolate both the camera constant, f, and the elevation of the exposure station, Z_o, as these parameters are strongly correlated. This lack of separation can be shown by investigating the "condition" of the matrix.

In this chapter, therefore, methods for detecting and overcoming the problems of size and stability will be discussed.

3.01 Review of Matrix Inversion

Most texts on matrix algebra, e.g. Faddeev and Faddeeva[18], not only provide a rigorous explanation of the matrix inverse, but also provide numerous algorithms for computing the same. Furthermore, program libraries such as the IBM Scientific Subroutine Package[19] already provide the photogrammetrist with the necessary computer software for many of these algorithms, thereby greatly reducing his work.

However, once the core storage capacity of the computer is exceeded, then the photogrammetrist must again address himself to the problem of devising adequate computer software. Consider the matrix system $(A^T \Sigma_l^{-1} A)$ of normal equations. Classically, this is a banded system. However, in the event of either A or Σ_l^{-1} becoming full, then $A^T \Sigma_l^{-1} A$ is full. The case where Σ_l^{-1} is full rather than block diagonal is especially realistic when satellite orbital data are used to constrain the photostation coordinates.

Table 2 lists some important references pertaining to the solution of $(A^T \Sigma^{-1} A)^{-1}$. Figure 2 depicts diagrammatically the form of the normal equation matrix.

Table 2

Reference List Pertaining to the Solution of High Order Inverses

Matrix Type	Method Name	Reference
1	Partitioned Regression*	Brown[20,21]
2	Triple Block Method*	Snowden[22]
2	Elassal's General Algorithm*	Elassal[23]
3	Triangularization	Uotila[24], IBM[19]
4	Gauss-Jordan	Berezin and Zhidkov[25], IBM[19]
5	Partitioning	Faddeev and Faddeeva[18]
6	Successive Partitioning	Snowden[22], Berezin and Zhidkov[25]

*These methods use the same fundamental concepts and essentially differ only in name.

Figure 2

Some Common Normal Equation Forms

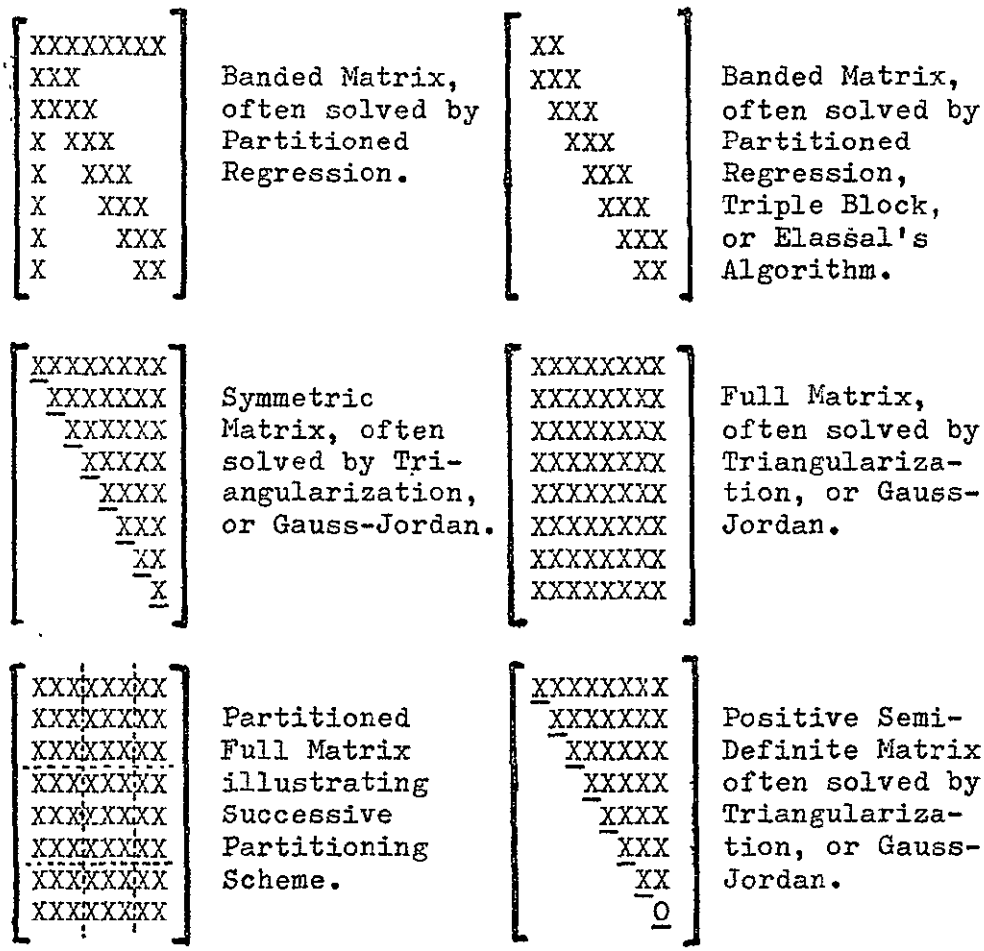

It is recognized that Table 2 is not complete and that the literature contains many other algorithms. One such algorithm that appears to be growing in importance is that used to "border" a matrix. This technique allows the use of the positive definite character of the matrix to the stage where the matrix becomes positive semi-definite (see Needham[26]).

3.02 Review of Solution Methods

As in the case of matrix inversion, a wealth of information can already be found in standard texts, e.g. Faddeev and Faddeeva[18], and in the journals. Unfortunately, most methods of solution depend on the normal equation matrix being positive definite, a feature that is destroyed when constraints are added to the system. However, these methods have usually proved to be superior to inverse techniques in both time and stability. Unfortunately, the variance-covariance matrix of the adjusted parameters is not easily obtained.

A complete description of the following methods can be found in either Faddeev and Faddeeva[18] or Berezin and Zhidkov[25]:

Gauss Elimination
Square Root Method
Gauss-Seidel
Relaxation

} These methods are normally used on symmetric- and full-type matrices, rather than on banded systems.

3.1 Vector and Matrix Norms

Since the concept of a vector norm is more easily envisaged and understood than that of a matrix norm, it is considered logical to develop the background for the n x 1 vector X before considering the more general matrix A of size n x m.

The norm of a vector is defined as a real, non-negative number, expressed as $\|X\|$ which represents, in some manner, the size of the vector X. The following three manipulative rules are important:

$$\|X\| \geq 0 \quad (\|0\| = 0, \text{ otherwise} > 0)$$
$$\|kX\| = \|k\| \cdot \|X\| \qquad (3.1)$$
$$\|X + Y\| \leq \|X\| + \|Y\|$$

Consider the following special cases for the n x 1 vector X:

(a) n = 1. In this case the size of X is best expressed by the modulus $|x|$. However, it is not the only estimator.

(b) n = 2. There is now no single number that accurately gives the size of such a vector. Some of the most logical and significant estimators are:

$$\|X\| = |x_1| + |x_2|$$
$$\|X\| = \left[|x_1|^2 + |x_2|^2 \right]^{1/2}$$
$$\|X\| = \max_{i=1,2} |x_i|$$

(c) n = 3. As the size of the vector increases, so does the number of logical and significant estimators. Some of these estimators are as follows:

$$\|X\| = |x_1| + |x_2| + |x_3|$$
$$\|X\| = \left[|x_1|^2 + |x_2|^2 + |x_3|^2 \right]^{1/2}$$
$$\|X\| = \left[|x_1|^3 + |x_2|^3 + |x_3|^3 \right]^{1/3}$$
$$\|X\| = \max_{i=1,2,3} |x_i|$$

From these examples it is readily seen that a general definition, the Hölder norm[27], is possible:

$$\|X\|_k = \left[\sum_{i=1}^{n} |x_i|^k \right]^{1/k} \qquad (3.2)$$

The term Euclidean norm is applied to the k = 2 norm, since it represents the length in multidimensional space from the point to the coordinate origin.

From the Hölder norm and from the above examples, it may readily be deduced that the following inequalities exist between the norms:

$$\|X\|_\infty \leq \|X\|_1 \leq n\|X\|_\infty$$
$$\|X\|_\infty \leq \|X\|_2 = \|X\|_E \leq \sqrt{n}\|X\|_\infty$$

It is now considered pertinent to consider norms associated with matrices and systems of linear equations. The basic algebraic rules which follow are similar to those for vector norms (equation set 3.1):

$$\begin{aligned}
&\|A\| \geq 0 \quad (\|0\| = 0, \text{ otherwise} > 0)\\
&\|kA\| = |k| \cdot \|A\|\\
&\|A + B\| \leq \|A\| + \|B\| \qquad (3.3)\\
&\|AB\| \leq \|A\| \cdot \|B\|\\
&\|AX\| \leq \|A\| \cdot \|X\|
\end{aligned}$$

Faddeev and Faddeeva[18] have shown that the following forms correspond to the equivalent vector norms. Thus, if the second norm is being used in vector work, then the associated second matrix norm must be used for associated matrix work.

$$\|A\|_1 = \max_j \left(\sum_{i=1}^{n} |a_{ij}|\right) \quad \text{- a column norm}$$

$$\|A\|_2 = \max (\lambda_i), \lambda_i \text{ of the matrix } A^T A \quad - A^T \text{ must be Hermitian}$$

$$\|A\|_\infty = \max_i \left(\sum_{j=1}^{n} |a_{ij}|\right) \quad \text{- a row norm}$$

It is obvious that the computational labour involved in $\|A\|_2$, the spectral norm, is immense. Therefore it has been common to use the more easily computed Euclidean norm, which is generally greater than the spectral norm by a factor of up to $\sqrt{n}$.

The Euclidean norm is

$$\|A\|_E = \left[\sum_{i=1}^{n}\sum_{j=1}^{n}|a_{ij}|^2\right]^{\frac{1}{2}} \qquad (3.4)$$

The following identities hold for matrix norms:

$$\|A\|_2 \leq \|A\|_E \leq \sqrt{n}\|A\|_2$$

$$\|A\|_2 \leq \left[\|A\|_1 \cdot \|A\|_\infty\right]^{\frac{1}{2}}$$

Two very common matrix norms are defined as follows:

$$M(A) = n \max_{i,j}|a_{ij}| \qquad (3.5)$$

$$N(A) = \left[\sum_{ij}|a_{ij}|^2\right]^{\frac{1}{2}} = \sqrt{\text{trace } A^T A} \qquad (3.6)$$

It is evident that the norm M(A) belongs to the $k = \infty$ class, while N(A) belongs to the $k = 2$ class. Some important relationships between norms are now given:

$$\frac{1}{n} M(A) \leq \|A\| \leq M(A)$$

$$\frac{1}{n} M(A) \leq \|A\|_1 \leq M(A)$$

$$\frac{1}{n} M(A) \leq \|A\|_2 \leq M(A)$$

$$\frac{1}{n} M(A) \leq N(A) \leq M(A)$$

$$\frac{1}{n} N(A) \leq \|A\|_2 \leq N(A)$$

$$\frac{1}{n} N(A) \leq \|A\| \leq \sqrt{n}\, N(A)$$

$$\frac{1}{n} N(A) \leq \|A\|_1 \leq \sqrt{n}\, N(A)$$

$$\frac{1}{n} \|A\|_2 \leq \|A\|_\infty \leq \sqrt{n}\, \|A\|_2$$

$$\frac{1}{n} \|A\|_2 \leq \|A\|_1 \leq \sqrt{n}\, \|A\|_2$$

$$\frac{1}{n} \|A\|_\infty \leq \|A\|_1 \leq n \|A\|_\infty$$

$$\left\|(I + C)^{-1}\right\| \leq \frac{1}{1-\|C\|}$$

$$\left\|I - (I + C)^{-1}\right\| \leq \frac{\|C\|}{1-\|C\|}$$

The last two inequalities are proved in Appendix C.

3.2 Stability Indicators and Test Matrices

Classically, four quantities are used to express the computational stability of a matrix system. These quantities are:

(a) The Turing[28] M and N numbers which are defined as:

$$M = \frac{1}{n} \cdot M(A) \cdot M(A^{-1}) \qquad (3.7)$$

$$N = \frac{1}{n} \cdot N(A) \cdot N(A^{-1}) \qquad (3.8)$$

(b) The Todd[29] P number, defined as:

$$P = \frac{\max|\lambda_i|}{\min|\lambda_i|}, \ \lambda_i \text{ of } A \qquad (3.9)$$

(c) The H number[18] defined as:

$$H = \sqrt{\frac{\max \lambda_i}{\min \lambda_i}}, \ \lambda_i \text{ of } A^T A \qquad (3.10)$$

It is well-known that these numbers tend to unity as the quality of the matrix increases. The limiting case occurs for

orthogonal matrices in which at least P = H = 1. Unfortunately, the upper limit is not bounded and therefore experience in working with systems becomes an important part of the decision process. Much of this experience is gained by experimenting with test matrices.

3.21 Orthogonal Test Matrices

It is possible to construct orthogonal matrices of any desired size for software testing. It is recognized that inverses computed via algorithms which ignore orthogonality should experience minimal roundoff error. This is due to the low magnitude of the stability numbers. However, such matrices seldom occur in Geodetic Science. A useful test form is given by Newman and Todd[30]:

$$A = (a_{ij}) \quad \text{where } a_{ij} = \sqrt{\frac{2}{n+1}} \cdot \sin\left(\frac{i \cdot j \cdot \pi}{n+1}\right)$$

and since A is orthogonal

$$A^T = A^{-1}$$

3.22 Ill-Conditioned Test Matrices

Just as it was possible to construct matrices with highly stable characteristics, it is also possible to construct matrices with highly unstable characteristics. A finite segment of the well-known Hilbert matrix and its variants have been shown to be highly unstable[30, 31, 32]. For instance, the P number associated with these matrices is approximately $e^{3.5\,n}$, where n is the order

of the matrix. Thus, this class of matrices, while not representative of the type of matrix normally encountered, offers the possibility of comparison between two given algorithms. The form of this matrix is as follows:

$$A = (a_{ij}) \quad \text{where} \quad a_{ij} = \frac{1}{i+j-1}$$

$$\text{then} \quad A^{-1} = (b_{ij}) \quad \text{where} \quad b_{ij} = \frac{(-1)^{i+j}(n+i-1)!\,(n+j-1)!}{(i+j-1)\left[(i-1)!\,(j-1)!\right]^2(n-i)!\,(n-j)!}$$

3.23 Some Tridiagonal Forms

Tridiagonal forms of the normal equation matrix do exist in Geodetic Science[33]. (For an example see Appendix D.) Furthermore, many tridiagonal forms have known eigenvalues and hence known P numbers, in addition to an algebraic inverse. It is this class of matrices which should be used to investigate computer software performance for geodetic applications. Gregory and Karney[34] list a number of suitable forms. However, experience has shown that the computational merits of a particular algorithm are not evident up to an order of at least n = 75. The reason for this is that the test matrices were positive definite and possessed uniformly small elements which could be exactly represented. Under such conditions, many algorithms will yield similar results,

e.g. for n = 70 and a tridiagonal matrix given by

$$A = (a_{ij}) \quad \text{where} \quad a_{ij} = 2,\ i = j$$
$$a_{ij} = 1,\ |i-j| = 1$$
$$a_{ij} = 0,\ |i-j| > 1$$

then $A^{-1} = \left(b_{ij}\right) = \frac{1}{n+1}\left(c_{ij}\right)$ where $c_{ij} = i(n-i+1),\ i = j$

$c_{ij} = c_{i,j-1} - i,\ j > i$

$c_{ij} = c_{ji},\ j < i$

Four representative methods yielded the following values for b_{11}:

Desk calculator	0.985 915 492 957 746 5
DSINV (IBM[19])	0.985 915 492 957 748
DMINV (IBM[19])	0.985 915 492 957 749
VERSOL (See Appendix E)	0.985 915 492 957 748

The P number for this problem is approximately 1985. Thus it is seen that, for this class and size of matrix, these inverse subroutines yield results with minimal roundoff error, despite the large P number.

3.24 A Test Matrix

A large matrix (370 x 370) resulting from the adjustment of gravity observations was available for testing. This matrix had gravity differences for its basic data. Thus, while the matrix was formed without any regard to a pattern, it could easily be condensed into a variant of the tridiagonal matrix. This matrix therefore became a convenient test matrix, as it was assumed to be a more representative matrix than the theoretical tridiagonal case due to the size of its elements as well as its order.

Since the matrix has an impressed condition, it was capable of being reduced into two variants. Table 3 shows the stability indicators for both variants. As mentioned earlier, no definitive

statements can be made regarding the quality of the matrix from these indicators, since they possess no upper bound. However, experience indicates that an acceptable solution to the inverse problem was obtained.

Table 3

Stability Indicators for the Test Matrix

Indicator	Variant 1 n = 369 (no imposed condition)	Variant 2 n = 370 (condition imposed)
M	$\sim 3.1 \times 10^4$	$\sim 9.2 \times 10^6$
N	$> 3.4 \times 10^3$	$> 1.2 \times 10^4$
P	4.2×10^4	5.5×10^6

3.3 Perturbation Theory

It was shown in Section 3.2 that the classical indicators are of limited use since they have no supremum. For this reason, other indicators of stability have been sought. A successful method based on the exact computation of a perturbed system is due to Wilkinson[35]. The method seeks to place bounds on the perturbations of the system necessary to perform a computation, rather than to follow the forward error propagation.

Consider the following matrix system:

$$AX + Y = 0 \qquad (3.11)$$

assuming that A is square with a non-zero determinant.

Then if A is perturbed by an amount E, X is perturbed by the vector δX such that the equation of the system becomes

$$(A + E)(X + \delta X) = -Y = Z \qquad (3.12)$$

or $$A(I + C)(X + \delta X) = Z \qquad (3.13)$$

where $AC = E$, which implies that, since A^{-1} exists, $C = A^{-1}E$. Alternatively, $\|C\| < 1$ is a sufficient condition (See Appendix C).

Solving for δX yields

$$\delta X = (I + C)^{-1} A^{-1} Z - X$$

but from equation (3.11) $X = A^{-1}Z$

Hence $$\delta X = \left[(I + C)^{-1} - I\right] X$$

Application of the norm theory to this expression yields

$$\|\delta X\| = \left\|\left[(I + C)^{-1} - I\right] X\right\| \leq \left\|\left[(I + C)^{-1} - I\right]\right\| \cdot \|X\|$$

$$\|\delta X\| \leq \left[\left\|(I + C)^{-1}\right\| + \|-I\|\right] \cdot \|X\|$$

$$\frac{\|\delta X\|}{\|X\|} \leq 1 + \left\|(I + C)^{-1}\right\| \leq \frac{\|C\|}{1 - \|C\|}$$

But $C = A^{-1}E$

Hence $$\frac{\|\delta X\|}{\|X\|} \leq \frac{\|A^{-1}E\|}{1 - \|A^{-1}E\|} \leq \frac{\|A^{-1}\| \cdot \|E\|}{1 - \|A^{-1}\| \cdot \|E\|} \qquad (3.14)$$

This last equation expresses, in terms of norms, the relative change in a solution vector due to a perturbation in the original matrix A, of size E. It must be stressed that the above expression is an inequality and that only an upper bound has been determined. This bound could be in considerable error if

$$\|A^{-1}E\| \ll \|A^{-1}\| \cdot \|E\|$$

It is important to note that the condition number is the decisive quantity in determining an upper bound. Consider a condition number defined as $k = \|A\| \cdot \|A^{-1}\|$

(note $M = \frac{1}{n} \cdot M(A) \cdot M(A^{-1})$ and $N = \frac{1}{n} N(A) \cdot N(A^{-1})$)

and a relative perturbation δ defined as $\delta = \frac{\|E\|}{\|A\|}$

Then the relative change can be expressed as

$$\frac{\|\delta X\|}{\|X\|} \leq \left[\|A^{-1}\| \cdot \|A\| \cdot \frac{\|E\|}{\|A\|}\right] \Big/ \left[1 - \|A^{-1}\| \cdot \|A\| \cdot \frac{\|E\|}{\|A\|}\right] = \frac{k\delta}{1-k\delta} \qquad (3.15)$$

Ordinarily δ is small, but if $k\delta \to 1$ due to large k, then $\frac{\|\delta X\|}{\|X\|} \to \infty$. This is critical in digital computers where δ is a fixed ratio.

It is possible to extend this perturbation theory[27] to include perturbation on the constant vector Y. Thus the perturbation equation (3.12) becomes

$$(A + E)\ (X + \delta X) = (Z + \delta Z) \qquad (3.16)$$

Application of the above theory yields the following equivalent expression to equation (3.14). Note $\|\delta Z\| = \|\delta Y\|$

$$\|\delta X\| \leq \frac{\|A^{-1}\| \cdot \|E\| \cdot \|X\| + \|A^{-1}\| \cdot \|\delta Y\|}{1 - \|A^{-1}\| \cdot \|E\|} \qquad (3.17)$$

The most efficient method of estimating $\|\delta X\|$ from a computational viewpoint is with the ∞ norm. The sacrifices in accuracy made with this norm can be determined, if desired, from the identities of Section 3.1. However, the physical significance of this norm is more important. Thus equation (3.17) becomes

$$\|\delta X\|_\infty \leq \frac{\|A^{-1}\|_\infty \cdot \|E\|_\infty \cdot \|X\|_\infty + \|A^{-1}\|_\infty \cdot \|\delta Y\|_\infty}{1 - \|A^{-1}\|_\infty \cdot \|E\|_\infty} \qquad (3.18)$$

It is to be noted that the following definitions apply to infinity norms which can be physically interpreted as row norms, since the maximum element vector norm is a degenerate case of the more general matrix row norm:

$\|X\|_\infty = \max|x_i|$ - maximum element norm

$\|A\|_\infty = \max_i \left(\sum_{j=1}^{n} |a_{ij}| \right)$ - row norm

The perturbation introduced in a digital computer when storing a number is given by $1:2^b$ where b is the number of bits in a word. For the IBM 360/75 of The Ohio State University Instruction and Research Computer Center (IRCC) the perturbation level is approximately 1 part in 10^7 for single precision and 1 part in 10^{15} for double precision. Thus, $\|E\|_\infty$ and $\|\delta Y\|_\infty$ are governed by the size of the elements of A and Y. For this discussion, it is convenient to view the perturbations as decimals. This is the situation which would exist if row and column normalization of the system were performed prior to solution. It is also convenient to use the double precision mode figures. Hence

$\|E\|_\infty = n \cdot 10^{-15}$

$\|\delta Y\|_\infty = 10^{-15}$

For the test matrix (Section 3.24), the following values of $\|A\|_\infty$ and $\|X\|_\infty$ were obtained:

$$n = 369, \quad \|A^{-1}\|_\infty = 1.2$$

$$n = 370, \quad \|A^{-1}\|_\infty = 44$$

$$\|X\|_\infty = 200$$

When these values are substituted into equation (3.18) together with the values of $\|E\|_\infty$ and $\|\delta Y\|_\infty$ the following are obtained:

$$n = 369, \quad \|\delta X\| \simeq 10^{-10}$$

$$n = 370, \quad \|\delta X\| \simeq 10^{-8}$$

This indicates that the solution vector is accurate to 10 significant figures for the $n = 369$ configuration and 8 significant figures for the $n = 370$ configuration. It therefore appears that the added condition did not strengthen the stability of the matrix. Moreover, the stability of the matrix is not a direct function of the P, N, and M numbers when the matrix is of a high order.

3.4 Matrix Refinement

This method, which is based on the control computation AA^{-1}, seeks to take an inverse which is known to possess roundoff errors and refine it until these errors are no longer of any computational consequence. The discrepancy between AA^{-1} and I is naturally an indicator of the degree of stability, for the closer AA^{-1} is to I, the more stable is the computation. Consider the following definition of the discrepancy matrix:

$$C_0 = I - AA_0^{-1} \tag{3.19}$$

It is immediately recognized that for A_0^{-1} to be an acceptable approximation to A^{-1}, then $|C_0| < k < 1$. The more easily com-

puted 1st and ∞ order norms are most commonly used, although Hotelling[36] introduced the concept of refinement using N(A). Faddeev and Faddeeva[18] show that the following relationship exists:

$$A_m^{-1} = A_{m-1}^{-1}(I + C_{m-1}) \tag{3.20}$$

Hence, from equation (3.19),

$$C_m = I - AA_m^{-1}$$

Expanding C_m yields

$$C_m = I - AA_{m-1}^{-1}(I + C_{m-1})$$

$$= I - (I - C_{m-1})(I + C_{m-1})$$

$$= C_{m-1}^2 = C_{m-2}^4 = \cdots \quad C_0^{2^m}$$

Hence,

$$A_m^{-1} = A^{-1}(I - C_0^{2^m}) \tag{3.21}$$

and in the limit, as $C_0^{2^m} \longrightarrow 0$, $A_m^{-1} \longrightarrow A^{-1}$.

This may be re-arranged to yield the following equation on which the computational algorithm has been built:

$$A_m^{-1} = 2A_{m-1}^{-1} - A_{m-1}^{-1}AA_{m-1}^{-1} \tag{3.22}$$

It is now desired that a single number, rather than the discrepancy matrix C, should indicate the quality of the computations. Thus, the concept of the norm must again be introduced.

Consider

$$D_m = A_m^{-1} - A^{-1}$$

then

$$\|D_m\| = \|A_m^{-1} - A^{-1}\| = \|-A^{-1}C_0^{2^m}\|$$

$$D_m = \left\| -A_{m-1}^{-1}(I - C_{m-1})^{-1} C_0^{2^m} \right\|$$

$$\leq |-1| \cdot \left\| A_m^{-1} \right\| \cdot \left\| (I - C_{m-1})^{-1} \right\| \cdot \left\| C_0^{2^m} \right\| \qquad (3.23)$$

and, in particular, if $m = 1$, $k = \left\| C_0 \right\|$

$$\left\| D_1 \right\| \leq \left\| A_0^{-1} \right\| \frac{k^2}{(1-k)} \qquad (3.24)$$

The test matrix of Section 3.24 was subjected to this refinement process. The initial and final values associated with the test matrix are listed in Table 4. The matrix was subjected to two refinement steps.

Table 4

Some Values for the Test Matrix Associated with Refinement

	$\left\| C_0 \right\|$		$\left\| D_m \right\|$	
	Initial	Final	Initial	Final
Variant 1 n = 369	4×10^{-11}	1×10^{-10}	2×10^{-20}	2×10^{-20}
Variant 2 n = 370	1.2×10^{-3}	2×10^{-10}	1.4×10^{-2}	4×10^{-18}

It is evident from Table 4 that only Variant 2 benefited from the refinement process. That is, the refinement process roundoff errors were themselves the limiting factor in the 369 x 369 case. However the 370 x 370 matrix, which was inverted by using the bordering technique on row 370, did respond to refinement. This response was due to the fact that the bordering

algorithm produced roundoff errors in excess of those restricting the refinement process.

A number of test examples of small to moderate order were tested, including finite segments of the Hilbert matrix. Results from these tests indicate that refinement is not possible for P levels in excess of 10^5, and that system instability occurs for P levels greater than 10^{10}.

These findings are consistent with those of Wilkinson[35], who shows that inequalities of the following type exist. (Note: With these inequalities, the quality of the initial approximation must be carefully considered.)

(a) Refinement occurs provided

$$\left\|A^{-1}\right\|_\infty \leq 2^{k-1}/n < 2^{-1}$$

where k is the number of machine bits in a word.

(b) The gain in precision in binary bits per iteration, m, is

$$n2^{-k}\left\|A^{-1}\right\|_\infty < 2^{-m}$$

(c) Component error level for residuals is approximately

$$\sqrt{n}\ 2^{j-k}$$

where 2^j is the maximum component of A^{-1}.

(Note: For first iteration, the level is $\sqrt{2}$ times above.)

(d) Error level in solution given by

$$(n)^{\frac{i}{2}}\ 2^{j-ik}\left[\left\|A^{-1}\right\|_\infty\right]^i$$

where i is the iteration.

Three examples illustrating these computations are listed in Table 5. These computations are pertinent to the IBM 360/75 of IRCC, where k = 56, hence $2^{56} \simeq 7.6 \times 10^{16}$ and $2^{-56} = 1.3 \times 10^{-17}$.

Table 5

Inequality Tests to Determine Possibility of Refinement

Matrix	$\|A^{-1}\|_\infty$	Refinement possible	Precision gain	Component error for residuals	Solution error i = 2
369 x 369	1.2	$\|A^{-1}\|_\infty = 1.2$ $2^{k-1}/n = 1.3 \times 10^{14}$ Yes	Yes	Small	Small
370 x 370	100	$\|A^{-1}\|_\infty = 100$ $2^{k-1}/n = 1.3 \times 10^{14}$ Yes	Yes	Small	Small
10 x 10 Hilbert segment	3×10^{13}	$\|A^{-1}\|_\infty = 3 \times 10^{13}$ $2^{k-1}/n = 7.6 \times 10^{15}$ Doubtful	Small gain possible	Significant (0.03)	Very great 10^9

Table 5 indicates that any instability in the systems would not become apparent until the second iteration if the initial inverse choice were good, since the errors present are not of sufficient size to unduly perturb the inverse.

However, when these errors are augmented with the larger errors of the refinement process, then an inverse quickly ceases to exist. When the refinement errors are of moderate size, or comparable to the roundoff error, oscillation takes place. Such an oscillating system was observed for the n = 6 segment of the Hilbert matrix.

Unfortunately, this technique may be impractical except in special circumstances, as central processing unit (CPU) time was 33 minutes per iteration for the 370 x 370 matrix. This time would certainly decrease with higher rates of information transfer between the disk unit and the core. The rate of transfer used in this problem was 312K bytes per second. Additionally, if a greater core region was used, then fewer calls to the IBCOM routines would also reduce CPU time. The present program required 16K bytes of core for storing the associated instructions. The necessary four work vectors require additional space which in this case amounted to 16K bytes. This space is determined by the order of the matrix.

The method could be useful in extending the core range of the machine, since it is theoretically possible to obtain a single precision inverse of limited quality, and thence to refine it to the desired level. However, care must be exercised to ensure that

the inverse is acceptable.

The program for accomplishing this work is listed in Appendix E.

3.5 Reinforcement

The principle of reinforcement is that the matrix A is considered as the last term of the following sequence:

$$A_0 = I,\ A_1,\ A_2 \cdots A_{k-1},\ A_k \cdots A_n = A$$

That is, matrix A_k is obtained by replacing the kth row of A_{k-1} with the kth row of A_k, thereby building up the desired matrix which at this juncture is unspecified.

The following derivation is due to Faddeev and Faddeeva[18]: Consider the matrix A to be non-singular and with known inverse, and consider the column vectors U and V defined such that

$$UV = \begin{bmatrix} u_1 \\ u_2 \\ \vdots \\ u_n \end{bmatrix} \begin{bmatrix} v_1, & v_2 \cdots v_n \end{bmatrix} = \begin{bmatrix} u_1v_1 & u_1v_2 \cdots u_1v_n \\ u_2v_1 & u_2v_2 \cdots u_2v_n \\ \cdots\cdots\cdots\cdots\cdots\cdots \\ u_nv_1 & u_nv_2 \cdots u_nv_n \end{bmatrix} \qquad (3.25)$$

Clearly, UV has rank 1, since every row of equation (3.25) is a linear combination of another row.

Then it has been shown by Dwyer and Waugh[37] that for the matrix

$$B = A + UV \qquad (3.26)$$

$$B^{-1} = A^{-1} - \frac{1}{1+VA^{-1}U} A^{-1}UVA^{-1} \qquad (3.27)$$

provided that $1 + VA^{-1}U \neq 0$

That is, it is possible to find the inverse of B, given a matrix A with known inverse which differs from B by a matrix of rank 1. In particular, if the UV matrix is constructed as

$$UV = \begin{bmatrix} 0 \\ 0 \\ 0 \\ \vdots \\ 1 \\ \vdots \\ 0 \end{bmatrix} \begin{bmatrix} v_1 & v_2 & \cdots & v_k & \cdots & v_n \end{bmatrix}$$

then only the elements of the kth row are being changed.

Using these concepts, equation (3.27) becomes

$$B^{-1} = A^{-1} - \frac{1}{1+Va_k} a_k(VA^{-1}) \qquad (3.28)$$

where a_k is the kth column of A^{-1}.

It is now recognised that VA^{-1} is a row vector resulting from a summation over a column. Hence, the following holds:

$$b_j = a_j - \frac{a_k(Va_j)}{(1+Va_k)} \qquad (3.29)$$

where b_j and a_j are the jth columns of A^{-1} and B^{-1} respectively.

Finally, the series concept is added, which provides a known inverse for A.

Thus, equation (3.29) becomes

$$b_j^{(k)} = b_j^{(k-1)} - \frac{b_k^{(k-1)} \, Vb_j^{(k-1)}}{1+Vb_k^{(k-1)}} \qquad (3.30)$$

which is the working algorithm for the solution of the inverse.

It should be noted that the only $B^{(k-1)}$ for which an inverse

is known is the identity matrix I. This matrix differs from the given matrix, A, by n rows of the form $(v_1\ v_2 \ldots v_k \ldots v_n)$. Hence, the kth vector of v's is the kth row of the given matrix, with the exception that the kth element must be zero to maintain the desired linear relationships. Thus,

V becomes $V_k = (a_1\ a_2 \ldots a_{k-1}, 0, a_{k+1}, \ldots a_n)_k$

It therefore becomes necessary to pre-multiply A by E_2-type elementary transformations to achieve unit diagonal terms to satisfy the above conditions. This, in turn, necessitates post-multiplication of B by E_2-type transformations to return the desired inverse. It is also noted that the method applies specifically to positive definite forms, which is a considerable drawback.

A computer program utilizing the above method is given in Appendix E. This program makes use of the disk storage and therefore may be used to invert any full positive definite matrix, since only six vectors of the order of the matrix are needed to accomplish the inversion.

Unfortunately, the method is very slow. Inversion of the 369 x 369 test matrix required 210 minutes of CPU time. Moreover, the number of significant digits obtained, when compared to the refined solution, was such that the process could be termed "unstable". Only four significant digits were obtained. Thus, it seems that until faster transfer rates can be realized together with increased word bit size, this method must be passed over as a mathematical curiosity.

3.6 Solution by the Square Root Method

This standard method of obtaining a solution vector is very stable for positive definite matrices and quite fast, computationally, on digital computers. Furthermore, since it is essentially a row process, it is readily adaptable for unlimited size by interlocking the auxiliary disk storage facility with the magnetic core. It can be extended to positive semi-definite matrices by simply defining A as a Hermitian matrix, rather than as a real matrix. Furthermore, this change of definition need not be invoked computationally until the positive definite character of the matrix is destroyed.

Consider the following matrix system:

$$AX + Y = 0$$

Then A can be triangularized such that $A = BB^T$

where B is triangular.

Then solve $B \cdot Z = -Y$ by substitution for Z

and finally $B^T X = Z$ by substitution to determine X, the solution vector.

In the above,

$$B = (b_{ij}) = \left[a_{ii} - \sum_{j=1}^{i-1} b_{ij}^2 \right]^{1/2} \qquad (i > 1)$$

$$= \left[\frac{a_{ij} - \sum_{k=1}^{i-1} b_{ik} b_{jk}}{b_{ii}} \right] \qquad (j > i)$$

$$= 0 \qquad (i > j)$$

The main difficulty in this efficient procedure is that the variance-covariance matrix of the adjusted parameters is not determined. Thus, other methods of determining the inverse must be undertaken.

3.7 The Monte Carlo Method

> ... The Monte Carlo method may briefly be described as the device of studying an artificial stochastic model of a physical or mathematical process. The device is certainly not new. Moreover, the theory of stochastic processes has been a subject of study for quite some time, and the novelty lies rather in the suggestion that where an equation arising in a nonprobabilistic context demands a numerical solution not easily obtainable by standard numerical methods, there may exist a stochastic process with distributions or parameters which satisfy the equation, and it may actually be more efficient to construct a process and compute the statistics than to attempt to use those standard methods ...
>
> Householder[38]

The Monte Carlo method appears to offer a convenient method of overcoming the lack of an inverse when a solution method is used. The theory and development of Oswald[39] was converted for application to the IRCC system, but as yet suitable and consistent results have not been obtained on medium scale test matrices. The reasons for this are likely to be many, but the problem appears to lie in the random number generator or its application.

At present, several thousand walks are required for 3 and 4 digit accuracies, thus giving rise to fairly lengthy execution times. A reduction in calls to the random number generator and better random numbers would materially aid in the solution of these problems. However, for the moment, this task does not

warrant further pursual, although it should not be forgotten.

An interesting aspect of the Monte Carlo method is that if the finite variance condition is fulfilled, as it must be for an inverse to be obtained, then roundoff error plays an extremely small part in the computational process. Rather, the limiting factor appears to be the number of walks necessary to achieve a desired level for the elements of the variance-covariance matrix. In many cases, three significant digits would suffice.

3.8 Conclusions

In summary, it is to be noted that the inversion methods investigated in this chapter do not appear to approach the speed or accuracy of those commonly used and mentioned in the review. However, this should not foreclose the possibility of further work on this subject. In particular, methods for quickly and accurately obtaining elements of the variance-covariance matrix associated with a solution vector should receive attention. The Monte Carlo method is but one suitable method which may be able to yield suitable results in moderate CPU times.

With regard to the problem of stability, it has been forcibly pointed out that the classical indicators are of limited use and, in general, it is far better to compute the norm of the solution vector and to compare this norm with the required precision levels. Should the precision of the solution be unacceptable, then refinement may be attempted, if feasible, or another solution tried. Alternatively, the computational stability of the matrix may be

improved by applying suitable constraints to the normal equation set. This may upset the positive definite nature of the matrix, but this is of no great importance. Should the stability decrease, then critical consideration should be given to the desirability and necessity for the constraint, and to the efficiency of the computational process used.

4. NUMERICAL TESTING

4.0 Introduction

In Chapter 2 the augmented collinearity condition equations (2.5) were proposed. Chapter 3 developed a number of numerical concepts and tests to provide a rigorous mathematical basis for determining whether or not the collinearity conditions can be satisfactorily augmented with additional parameters. It is therefore the purpose of this chapter to link the previous two sections by means of numerical tests as well as by a clear demonstration of the advantages of the augmented system.

Two principal methods of testing are available to research workers. The first method involves testing with simulated data. In essence, this method consists of mathematically generating artificial point data according to some defined relationships, then using this data to test and check the new functions and associated computer software. The resulting estimated parameters may be compared against the true or known values of the parameters.

The second method uses real data derived from the observation process. The parameters estimated in this way cannot be compared against known standard values, since these do not exist. The ultimate object of the method is the determination of these unknown parameters to within a given confidence interval. The smaller the

given confidence interval, the more accurately is the unknown parameter determined.

In general, the first method allows a greater variety of tests to be made. However, there is always a small probability that the simulated data conform to the proposed model, whereas the real data are not represented by the proposed model. Thus model testing is not complete without real data tests, even though tremendous insight and understanding may be gained when simulated data are used. Unfortunately, real data are often most difficult to obtain, and even more difficult to implement initially. The Lunar Orbiter IV mission is not an exception in these matters, as contractual difficulties have delayed the furnishing of such real data. Thus only simulated tests can be described in this report.

The tests to be described in this chapter fall into two categories. The first is concerned with single photo tests, while the second section builds the single photo tests into a multiple photo block.

4.1 Generating the Simulated Data

The well-known collinearity condition equations (2.1) have long been recognised as the mathematical expressions by which object space points are connected to image space points by way of the lens nodal points. It was therefore natural to choose these equations as the basis on which the simulated data were generated.

The object space field was selected from the Department of

Defense Selenodetic Control System 1966[1]. It consisted of all points between 0°N and 30°N and between 10°W and 10°E. These points were then transformed into a right-handed X, Y, Z cartesian system. The selected object space field roughly corresponds to the area recorded on photographs numbered 109 and 102 of Lunar Orbiter IV. Figure 3 illustrates the area chosen and the limits of the photographic coverage.

Photostation positions approximating the position of exposures 109 and 102 were computed in the X, Y, Z system, together with attitudes in the omega, phi, kappa rotation system. It was therefore possible to compute the corresponding image coordinates for each object point at each of the two assumed photostations for a 610 mm focal length system. Figure 4 illustrates the density and location of image points for a photograph similar to photo number 109. The same object space field was transformed into an image space for slightly different photostations corresponding to pseudo-velocities. Next, the image space was split into eleven equal sections corresponding to a Δt time interval of 0.01 sec. It was assumed that the focal plane shutter progressed from positive y to negative y at a rate of 1 m/sec. The positions of those points which fell in a particular Δt interval were therefore computed for the photostation corresponding to that pseudo-velocity times Δt. The initial epoch, $\Delta t = 0$, was assumed to occur when the shutter crossed the midpoint of the image space. This is illustrated in Figure 4.

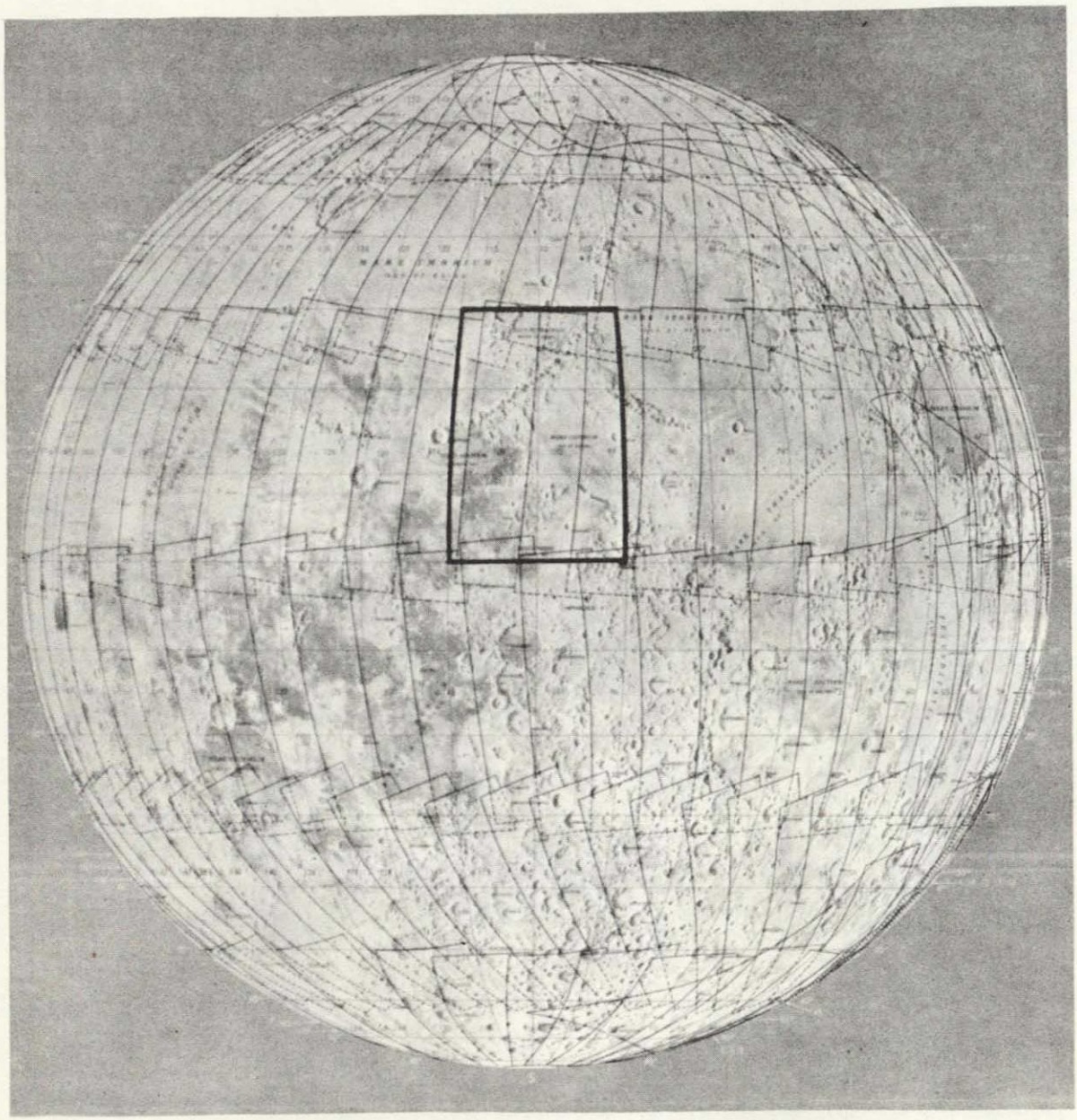

FIGURE 3

LUNAR ORBITER IV PHOTO INDEX
(NEAR SIDE)
WITH OUTLINE OF AREA USED IN
GENERATING THE SIMULATED DATA

FIGURE 4

TYPICAL SET OF SIMULATED DATA POINTS ILLUSTRATING THE UNIFORM DISTRIBUTION AND THE ELEVEN 0.01 SEC. EPOCHS INTO WHICH THE PHOTOGRAPH WAS DIVIDED

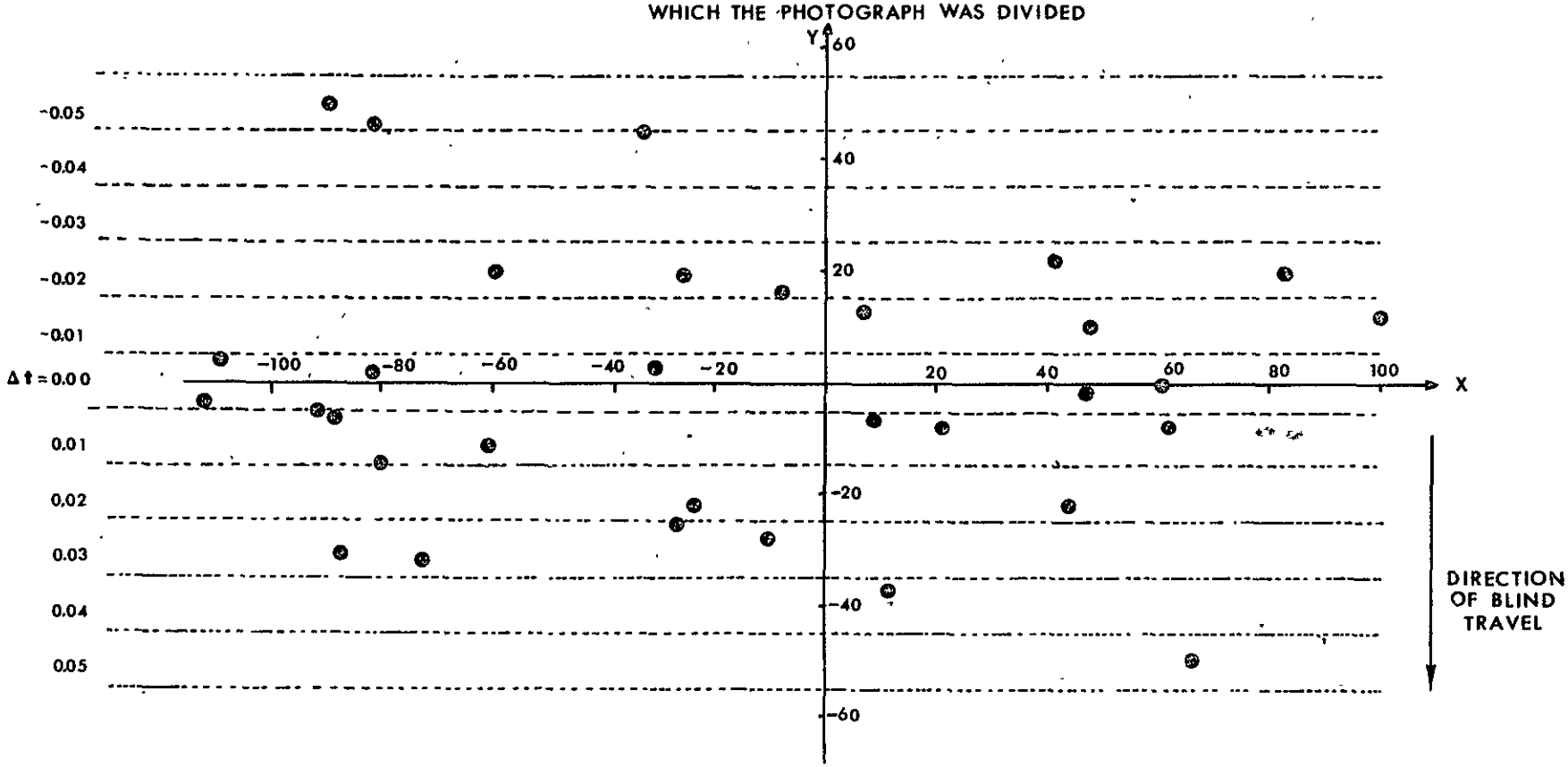

Thus an image space field with a corresponding object space field was constructed without resorting to the proposed model, although the concepts are similar. As is the case with such simulated data, the determined parameters possessed true values against which they could be tested. The total number of points in the object test area was 46, 32 of which are shown in Figure 4. The exact number and location of points used varied from test to test, depending on the particular requirements of the test.

4.2 Single Photo Tests - The Resection Problem

Usually space resection problems are concerned only with the elements of exterior orientation. However, in the case of the Lunar Orbiter missions where the coordinates of the principal point must be considered as unknown, it is necessary to include these quantities amongst the unknown parameters or quantities to be adjusted. Furthermore, there is evidence to suggest that these quantities are not fixed, unlike the case of frame cameras used in conjunction with recoverable film. It is therefore convenient for the purpose of this study to consider the unknown coordinates of the principal point as part of the exterior orientation elements.

There are three principal subdivisions to the space resection problem. These subdivisions are made according to the amount of observational data that are available. They are as follows:-

Case (a), characterized by - observations on photopoints.

Case (b), characterized by - observations on photopoints.
- observations on elements of exterior orientation.

Case (c), characterized by - observations on photopoints.
- observations on elements of exterior orientation.
- observations on survey points.

4.21 Case (a)

In accordance with the above description of this case, the general mathematical system $F(L_a, X_a) = 0$ was chosen. This expression is linearized according to the usual Taylor series expansion method to yield:

$$AV + B\Delta + \epsilon = 0 \qquad (4.1)$$

In this case,

$$A = \begin{bmatrix} \frac{\partial F_{1p}}{\partial x_p} & \frac{\partial F_{1p}}{\partial y_p} \\ \frac{\partial F_{2p}}{\partial x_p} & \frac{\partial F_{2p}}{\partial y_p} \end{bmatrix} = \begin{bmatrix} 1 & 0 \\ 0 & 1 \end{bmatrix} = I$$

Hence, (4.1) becomes

$$V + B^{E}\Delta^{E} + \epsilon = 0$$

The system is completely general for n points. Under such conditions, the dimensions are as follows,

$$\underset{(2n \times 1)}{V} + \underset{(2n \times 6)}{\overset{E}{B}} \cdot \underset{(6 \times 1)}{\overset{E}{\Delta}} + \underset{(2n \times 1)}{\epsilon} = 0 \qquad (4.2)$$

and the solution or correction vector is the well-known form

$$\overset{E}{\Delta} = -\left[\overset{E}{B}^T P \overset{E}{B}\right]^{-1} \overset{E}{B}^T P \overset{E}{\epsilon} \qquad (4.3)$$

The correction vector Δ is now added to the approximate value vector X_{oo} and the process repeated until the correction vector is small. A complete description of this elementary adjustment procedure is given by Richardus[40] and Uotila[24], among others.

4.22 Case (b)

This case was first described by Brown[41,42] in 1959 and subsequently fully detailed in 1964. There are two observation sets with the same unknown parameters. These sets can be symbolically written as follows:

$$\begin{aligned} F(L_a^1, X_a) &= 0 \\ G(L_a^2, X_a) &= 0 \end{aligned} \qquad (4.4)$$

The first set of observations results from plate observations and uses the collinearity conditions, equation set (2.5), as the mathematical function. The second equation set originates from observations on the elements of exterior orientation. These observations are made to conform to the following concept under minimum variance:

$$Y_{ai} - X_{ai} = 0$$

where X_{ai} is the adjusted or theoretical value of the parameter i,

Y_{ai} is the adjusted observation on the parameter i,

and i is the parameter x_o, y_o, ω, ϕ, κ ....

The solution of such a set of equations follows a well-defined routine, commencing with the linearization of the two symbolic matrix equations:

$$\begin{aligned} A_1 V_1 + B_1 \overset{E}{\Delta} \overset{E}{} + \epsilon_1 &= 0 \\ A_2 V_2 + B_2 \overset{E}{\Delta} \overset{E}{} + \epsilon_2 &= 0 \end{aligned} \qquad (4.5)$$

It is noted that by definition $A_1 = I$ and $A_2 = I$, and that $\overset{E}{B}_2 = -I$. Hence the observations can be represented by

$$\begin{aligned} V_1 + \overset{E}{B}_1 \overset{E}{\Delta} + \epsilon_1 &= 0 \qquad - \text{ 2n equations} \\ V_2 - \overset{E}{\Delta} + \epsilon_2 &= 0 \qquad - \text{ 14 equations} \end{aligned} \qquad (4.6)$$

The minimum variance solution of these two equations is obtained by minimizing the variables V_1, V_2 and $\overset{E}{\Delta}$ in the following function:

$$\begin{aligned} \phi = V_1^T P_1 V_1 + V_2^T P_2 V_2 - 2\lambda_1^T (V_1 + \overset{E}{B}_1 \overset{E}{\Delta} + \epsilon_1) \\ - 2\lambda_2^T (V_2 - \overset{E}{\Delta} + \epsilon_2) = 0 \end{aligned} \qquad (4.7)$$

Differentiation with respect to the variables in (4.7) yields:

$$\frac{\partial \phi}{\partial V_1} = 2P_1V_1 - 2\lambda_1$$

$$\frac{\partial \phi}{\partial V_2} = 2P_2V_2 - 2\lambda_2$$

$$\frac{\partial \phi}{\partial \overset{E}{\Delta}} = -2\overset{E_T}{B_1}\lambda_1 + 2\lambda_2$$

Hence, the necessary information for a solution is as follows:

$$V_1 + \overset{E}{B_1}\overset{E}{\Delta} + \epsilon_1 = 0$$

$$V_2 - \overset{E}{\Delta} + \epsilon_2 = 0$$

$$P_1V_1 - \lambda_1 = 0 \qquad (4.8)$$

$$P_2V_2 - \lambda_2 = 0$$

$$\overset{E_T}{B_1}\lambda_1 - \lambda_2 = 0$$

This equation set can be simplified by substituting the first lines into the last line from which λ_1 and λ_2 have been removed by substitution of lines 3 and 4. That is,

$$V_1 = -(\overset{E}{B_1}\overset{E}{\Delta} + \epsilon_1)$$

$$V_2 = -(-\overset{E}{\Delta} + \epsilon_2)$$

are substituted into

$$\overset{E_T}{B_1}P_1V_1 - P_2V_2 = 0$$

which yields

$$\overset{E_T}{B_1}\, P_1(-\overset{E}{B_1}\,\overset{E}{\Delta} - \epsilon_1) + P_2(-\overset{E}{\Delta} + \epsilon_2) = 0$$

Simplification yields

$$(\overset{E_T}{B_1}\, P_1\, \overset{E}{B_1} + P_2)\overset{E}{\Delta} + \overset{E_T}{B_1}\, P_1 \epsilon_1 - P_2 \epsilon_2 = 0$$

$$\text{or } \overset{E}{\Delta} = -(\overset{E_T}{B_1}\, P_1\, \overset{E}{B} + P_2)^{-1}\ (\overset{E_T}{B_1}\, P_1 \epsilon_1 - P_2 \epsilon_2) \qquad (4.9)$$

The corrections are applied and a new iteration commenced with the updated approximate value vector, X_{oo}.

Uotila[43] has suggested the following alternative computational algorithm:

Lines 2 and 3 of (4.8) may be expressed as

$$\overset{E}{\Delta} = V_2 + \epsilon_2$$

$$V_1 = P_1^{-1} \lambda_1$$

Substitution of these into line 1 yields

$$P_1^{-1} \lambda_1 + \overset{E}{B_1}(V_2 + \epsilon_2) + \epsilon_1 = 0 \qquad (4.10)$$

Similarly, line 5 of (4.8) may be expressed as

$$\lambda_2 = \overset{E_T}{B_1}\, \lambda_1$$

which can be substituted into line 4 to yield

$$P_2 V_2 - \overset{E_T}{B_1}\, \lambda_1 = 0 \qquad (4.11)$$

Regrouping equations (4.10) and (4.11) yields

$$\begin{bmatrix} P_1^{-1} & \overset{E}{B_1} \\ \overset{E_T}{B} & -P_2 \end{bmatrix} \begin{bmatrix} \lambda_1 \\ V_2 \end{bmatrix} = \begin{bmatrix} \overset{E}{-B_1}\epsilon_2 - \epsilon_1 \\ 0 \end{bmatrix} \tag{4.12}$$

The solution to this equation set in terms of V_2 is as follows:

$$\begin{aligned} V_2 &= \left[-(-P_2 - \overset{E_T}{B_1} P_1 \overset{E}{B_1})^{-1} \overset{E_T}{B_1} P_1\right]\left[-(\overset{E}{B_1}\epsilon_2 + \epsilon_1)\right] \\ &= -(\overset{E_T}{B_1} P_1 \overset{E}{B_1} + P_2)^{-1} \overset{E_T}{B_1} P_1 (\overset{E}{B_1}\epsilon_2 + \epsilon_1) \end{aligned} \tag{4.13}$$

This is normally further simplified by assuming that X_{oo}, the approximate value vector, equals L_b, the observation vector. Under such assumptions, equation (4.13) reduces to

$$V_2 = -(\overset{E_T}{B_1} P_1 \overset{E}{B_1} + P_2)^{-1} \overset{E_T}{B_1} P_1 \epsilon_1 \tag{4.14}$$

A new approximate value vector may be computed as $X_{oo} = L_b + V_2$, the respective partials re-evaluated, and a new residual vector for V_2 computed according to (4.13). This process is continued until the residuals meet prescribed limits or become constant.

4.23 Case (c)

Case (c) is a further generalization of case (b). This generalization is achieved by adding a third set of observations on the object space points. Thus the system now becomes

$$F(L_a^1, X_a) = 0$$

$$G(L_a^2, X_a) = 0 \qquad (4.15)$$

$$H(L_a^3, X_a) = 0$$

The last set of observations, which may be viewed as a further set of conditions, is extremely powerful, for now the object space point, the lens point and the image point are free to move so that the collinearity condition is fitted in a minimum variance manner at three points on the ray under consideration. Since only two points in space are necessary to define a line, any additional points along the line do not contribute further information. However all observations are subject to errors, and some observations are more easily and more precisely obtained than others. The incorporation of the additional information, by minimum variance techniques, into a general model, allows the least precisely observed quantities to be determined with a precision approaching that of the quantities defining the line. Since the most difficult and expensive observations are usually those associated with the object space, it is possible to relax the precision requirements on these quantities by enforcing the collinearity condition in this general manner.

Linearization of equation set (4.15) yields:

$$\begin{aligned} A_1 V_1 + B^E \overset{E}{\Delta} + B^S \overset{S}{\Delta} + \epsilon_1 &= 0 \\ A_2 V_2 + B_2 \overset{E}{\Delta} + \epsilon_2 &= 0 \\ A_3 V_3 + B_3 \overset{S}{\Delta} + \epsilon_3 &= 0 \end{aligned} \qquad (4.16)$$

which is readily simplified, by virtue of

$$A_1 = I,\ A_2 = I,\ A_3 = I,\ B_2 = -I,\ B_3 = -I,$$

to

$$\begin{aligned} V_1 + B^E \overset{E}{\Delta} + B^S \overset{S}{\Delta} + \epsilon_1 &= 0 \\ V_2 - \overset{E}{\Delta} + \epsilon_2 &= 0 \\ V_3 - \overset{S}{\Delta} + \epsilon_3 &= 0 \end{aligned} \qquad (4.17)$$

The solution of such a system of equations is exactly analogous to that discussed in Section 4.22 for case (b). It therefore suffices to write the solution as follows:

$$\left[\begin{array}{cc:cc} E_T & E & E_T & S \\ B^T P_1 & B + P_2 & B^T P_1 & B \\ \hdashline S_T & E & S_T & S \\ B^T P_1 & B & B^T P_1 & B + P_3 \end{array}\right] \left[\begin{array}{c} E \\ \Delta \\ \hdashline S \\ \Delta \end{array}\right] + \left[\begin{array}{c} E_T \\ B^T P_1 \epsilon_1 - P_2 \epsilon_2 \\ \hdashline S_T \\ B^T P_1 \epsilon_1 - P_3 \epsilon_3 \end{array}\right] = 0 \qquad (4.18)$$

It is evident that as $P_3 \rightarrow 0$, then case (c) is reduced to case (b), and that as $P_2 \rightarrow 0$ further restrictions reduce case (b) to case (a).

4.24 Numerical Results

Since the commonly-used collinearity condition techniques may be applied to the numerical solution of the theoretical models discussed in Section 4.23, it is not considered pertinent to present here a detailed discussion of the numerical methods. However, unique features of these numerical solutions, e.g. the analytical differentiation of the partials, may be found in Appendix F.

4.241 Case (a)

Two principal classes of tests were performed in this case. The first class involved points where the exposure epoch differed by a constant amount from the tracking epoch. It was assumed that all points were exposed simultaneously by a camera system using a between-the-lens type shutter system. The second class of tests involved points imaged at differing times corresponding to the passage of a focal plane shutter across the image area.

It was quickly recognised that while solutions can be obtained with the P = I unit weight concept, the quality of these solutions leaves much to be desired. In a class one test with unit weight, an acceptable determination for the unknown parameters was obtained. However the variance-covariance matrix of the adjusted parameters had exceedingly large norms, of the order of 10^{24} for $\|N^{-1}\|_\infty$ Furthermore, the symmetric characteristics of this matrix had been destroyed. The large value for the infinity norm can be directly attributed to the fact that no row-column normalization was per-

formed prior to inversion. When the correct weight matrix, $P = 10^{12} \cdot I$, was used, the order of the infinity norm was reduced to 10^{12}, while the symmetric characteristics of the variance-covariance matrix were retained. By applying the correct weight matrix, some degree of normalization is achieved, and this results in better computational stability.

Class two tests all yielded very satisfactory determinations of the unknown parameters. The quality of the determination was, however, dependent on a number of factors. Of these, the most important was the knowledge of Δt for a point. As indicated previously, the image space was sectioned into eleven regions, each of $\Delta t = 0.01$. This allowed an image smear of approximately 5 micrometers in x and 1 micrometer in y. However these values were not considered unreasonable, since blind velocity was a nominal 1000 mm/sec, compared with 1200 mm/sec for Lunar Orbiter IV. The quality of the determination increased as Δt for a point became more refined. This refinement was achieved by reducing the slit width. It therefore seems that increasing the exposure interval by increasing the slit width is less desirable than reducing the velocity of the blind, even though this will increase geometric distortion. It was also found that the initial approximations to the unknown parameters had to be reasonable, otherwise no convergence occurred due to the non-linearity of the model.

The principal results of case (a) tests are summarized in Table 6.

Table 6

Summary of Case (a) Numerical Results

	Parameter	Simulated Values	Class 1	Class 2 (5μm smear)
Principal Point	x_o (mm)	0.2000	0.1999	0.1996
	y_o (mm)	0.2000	0.1998	0.1997
Photostation Position	X (m)	4320000.	4320000.	4320000.
	Y (m)	-200000.	-200000.	-200000.
	Z (m)	922000.	922000.	921999.
Camera Attitude	κ (deg)	0.0	0.	0.
	ϕ (deg)	80.0	80.	80.
	ω (deg)	10.0	10.	10.
Photostation Velocities	V_x (m/sec)	100.0	159.	97.
	V_y (m/sec)	-100.0	-99.	-106.
	V_z (m/sec)	2000.	2003.	2008.
Camera Attitude Velocities	$\dot{\kappa}$ (^{o}/sec)	0.0	0.	0.
	$\dot{\phi}$ (^{o}/sec)	0.0	0.	0.
	$\dot{\omega}$ (^{o}/sec)	0.0	0.	0.
$\|N^{-1}\|_\infty$			$\sim 10^{14}$	$\sim 10^{13}$

4.242 Case (b)

This class of tests was concerned with the effects of weighting the unknown parameters by observations on the parameters. It was possible to test with a wide range of weights, both reasonable and unreasonable.

It is known from elementary adjustment theory that $P = m_o^2 \sum_{L_b}^{-1}$, and under the assumption that $m_o^2 = 1$ and that $\sum_{L_b}$ is diagonal, then P is also diagonal with elements according to $P_{ii} = \frac{1}{\sigma_{ii}} = \frac{1}{\sigma_i^2}$.

The use of reasonable weights greatly improved the stability of the system, when compared to case (a). The results of an unreasonable case are tabulated in Table 7, from which it is readily seen that excellent agreement between the simulated values and the adjusted values is possible. In the tabulated example, the position of the principal point and the attitude of the camera can be considered as known quantities to which almost no correction can be applied. It is most enlightening to compare the norms for these severe cases with those for case (a) tests. However, due to the number of variables involved, it is too difficult to display the reduction in size as a function of increased knowledge of the unknown parameters. It therefore must suffice to say that dramatic changes in stability occur when observations on some of the unknown parameters can be incorporated into the model.

Table 7

An Example of Case (b) Results

	Parameter	Precision of Observation ±	Weight	Simulated Values	Adjusted Values
Plate Coordinates	x_p (mm)	10^{-3}	10^6		
	y_p (mm)	10^{-3}	10^6		
Principal Point	x_o (mm)	0.001	10^6	0.2000	0.2000
	y_o (mm)	0.001	10^6	0.2000	0.2000
Photostation Position	X (m)	3	10^{-1}	4320000.	4320000.
	Y (m)	3	10^{-1}	-200000.	-200000.
	Z (m)	3	10^{-1}	922000.	922000.
Camera Attitude	κ (rad)	0.001	10^6	0.0	0.0
	ϕ (rad)	0.001	10^6	80.0	80.0
	ω (rad)	0.001	10^6	10.0	10.0
Photostation Velocities	V_x (m/sec)	10	10^{-2}	100.	100.
	V_y (m/sec)	10	10^{-2}	-100.	-100.
	V_z (m/sec)	10	10^{-2}	2000.	2000.
Camera Attitude Velocities	$\dot{\kappa}$ (rad/sec)	0.01	10^4	0.0	0.0
	$\dot{\phi}$ (rad/sec)	0.01	10^4	0.0	0.0
	$\dot{\omega}$ (rad/sec)	0.01	10^4	0.0	0.0
$\|N^{-1}\|_\infty$					10^7

4.243 Case (c)

Tests on this case were done in conjunction with the multiple photo tests, since n = 1 is a special case of the general n x m photo block. The principal difference is that observations are now available on all quantities. As would be expected from the previous discussion, good solutions with stable inverses are possible under a wide range of conditions. In particular, if the weights of the observed quantities are correctly entered then, since the expected value of m_o^2 is 1, the variance-covariance matrix of the adjusted quantities is approximately known. The upper bound of the matrix norm $\|A^{-1}\|_\infty$ can be estimated to be the quantity $n.\max_i(a_{ii}^{-1})$, since correlation is $\leq |1|$. Consequently, for this case, the quality of the solution can be estimated prior to execution and, if warranted, precautions taken to ensure that an acceptable solution is obtained.

The reader is referred to Section 4.3 for numerical data.

4.3 The n x m Photo Block - The Intersection Problem

The case of the intersection problem is built upon the single photo resection problem. Associated with each photograph is a set of observations on plate coordinates symbolically expressed as

$$\begin{aligned} F(L_a^{1a}, X_a) &= 0 \\ F(L_a^{1b}, X_a) &= 0 \\ &\vdots \\ F(L_a^{1i}, X_a) &= 0 \end{aligned} \qquad (4.19)$$

which can be expressed as

$$D(L_a^1, X_a) = 0$$

The same concept can be extended to observations associated with the elements of exterior orientation:

$$\begin{aligned} G(L_a^{2a}, X_a) &= 0 \\ G(L_a^{2b}, X_a) &= 0 \\ &\vdots \\ G(L_a^{2j}, X_a) &= 0 \end{aligned} \qquad (4.20)$$

Again, this system can be simplified by using the matrix equation

$$E(L_a^2, X_a) = 0$$

Finally, the observations on the survey coordinates can be expressed as

$$H(L_a^3, X_a) = 0 \qquad (4.21)$$

Thus, the matrix system associated with the intersection problem may be expressed as

$$\begin{aligned} D(L_a^1, X_a) &= 0 \\ E(L_a^2, X_a) &= 0 \\ H(L_a^3, X_a) &= 0 \end{aligned} \qquad (4.22)$$

which corresponds to equation set (4.15) of Section 4.23. The solution to equation set (4.15), namely (4.18), is therefore also the solution to (4.22). However the sub-blocks are now built from data associated with more than one photograph. It is therefore

considered pertinent to restate the solution to equation set (4.19) and then to discuss the composition of the sub-blocks in this new context.

$$\left[\begin{array}{c|c} {}^{E_T}_{B}P_1\ {}^{E}_{B} + P_2 & {}^{E_T}_{B}P_1\ {}^{S}_{B} \\ \hline {}^{S_T}_{B}P_1\ {}^{E}_{B} & {}^{S_T}_{B}P_1\ {}^{S}_{B} + P_3 \end{array}\right]\left[\begin{array}{c} {}^{E}\Delta \\ \hline {}^{S}\Delta \end{array}\right] + \left[\begin{array}{c} {}^{E_T}_{B}P_1\epsilon_1 - P_2\epsilon_2 \\ \hline {}^{S_T}_{B}P_1\epsilon_1 - P_3\epsilon_3 \end{array}\right] = 0 \qquad (4.23)$$

The segment ${}^{E_T}_{B}P_1\ {}^{E}_{B} + P_2$ is formed by augmenting equation set (4.19) with equation set (4.20). It is noted that the elements of exterior orientation appear only in functions concerned with a particular photo. That is, the differentials of elements of photo i are zero except in photo i. The following matrix describes the situation for a two photo case:

$${}^{E_T}_{B}P_1\ {}^{E}_{B} + P_2 =$$

$$\left[\begin{array}{cc} \underset{(14x2n)}{{}^{E_T}_{B_{1a}}} \cdot \underset{(2nx2n)}{P_1} \cdot \underset{(2nx14)}{{}^{E}_{B_{1a}}} + \underset{(14x14)}{P_{2a}} & 0 \\ 0 & \underset{(14x2n)}{{}^{E_T}_{B_{1b}}} \cdot \underset{(2nx2n)}{P_1} \cdot \underset{(2nx14)}{{}^{E}_{B_{1b}}} + \underset{(14x14)}{P_{2b}} \end{array}\right]$$

The sub-element ${}^{S_T}_{B}P_1\ {}^{S}_{B} + P_3$ is a square 3n x 3n matrix formed by augmenting equation set (4.19) with (4.21). Unlike the exterior elements, ground points are not confined to imaging on a single

photograph. Hence, under the assumption that the points are uncorrelated, the sub-element may be expressed as follows:

$$\underset{(3nx2n)}{{}^{S_T}B} \cdot \underset{(2nx2n)}{P_1} \cdot \underset{(2nx3n)}{{}^{S}B} + \underset{(3nx3n)}{P_3} =$$

$$\begin{bmatrix} {}^{S_T}B_{1a} & {}^{S_T}B_{2a} & \cdots \end{bmatrix} \begin{bmatrix} P_{1a} & 0 & \cdots \\ 0 & P_{1b} & \cdots \\ \cdot & \cdot & \\ \cdot & \cdot & \\ \cdot & \cdot & \end{bmatrix} \begin{bmatrix} {}^{S}B_{1a} \\ {}^{S}B_{2a} \\ \cdot \\ \cdot \\ \cdot \end{bmatrix} + P_3 =$$

$${}^{S_T}B_{1a}\, P_{1a}\, {}^{S}B_{1a} + {}^{S_T}B_{1b}\, P_{1b}\, {}^{S}B_{1b} + \cdots \quad P_3$$

The sub-element ${}^{E_T}B\, P_1\, {}^{S}B$ and its transpose ${}^{S_T}B\, P_1\, {}^{E}B$ combine parts of the previous two sub-elements. It is readily seen that the dimensions of ${}^{E_T}B\, P_1\, {}^{S}B$ are

(no. of photos times 14 x 2n) . (2n x 2n) . (2n x 3n)

and hence

$${}^{E_T}B\, P_1\, {}^{S}B = ({}^{S_T}B\, P_1\, {}^{E}B)^T = \begin{bmatrix} {}^{E_T}B_{1a}\, P_1\, {}^{S}B_{1a} \\ {}^{E_T}B_{1b}\, P_1\, {}^{S}B_{1b} \\ \cdot \\ \cdot \\ \cdot \end{bmatrix}$$

Either by expansion or by applying the above principles to the U section of the normal equation matrix, it may readily be deduced

that the following equations hold:

$$\overset{E_T}{B}\, P_1 \epsilon_1 - P_2 \epsilon_2 = \begin{bmatrix} \overset{E_T}{B}_{1a}\, P_{1a} \epsilon_{1a} - P_{2a} \epsilon_{2a} \\ \overset{E_T}{B}_{1b}\, P_{1b} \epsilon_{1b} - P_{2b} \epsilon_{2b} \\ \vdots \\ \vdots \end{bmatrix}$$

$$\overset{S_T}{B}\, P_1 \epsilon_1 - P_3 \epsilon_3 = \overset{S_T}{B}_{1a}\, P_{1a} \epsilon_{1a} + \overset{S_T}{B}_{1b}\, P_{1b} \epsilon_{1b} + \cdots \quad P_3 \epsilon_3$$

The structure of both the normal equation matrix and the constant vector are unique under the special conditions of diagonal weight matrices. As the size of the matrices increases, this unique structure must be exploited more and more in order that the size of the problem does not outstrip the capabilities of the computing facilities. In the numerical work associated with the testing of this model, sufficient core was available so that partitioning schemes were not necessary.

4.31 Numerical Tests

The numerical tests associated with this section were performed on a block of two photographs. The photographic data were generated according to the method described in Section 4.1 for positions and attitudes approximating Lunar Orbiter IV photographs 102 and 109. The ground data and exterior orientation data necessary to accomplish the data generation process were then assumed to be equivalent to the required observation parameters.

The two photographs had a nominal 60% overlap with a total of 24 ground points appearing in the overlap area. For convenience, it was assumed that the variance-covariance matrices for the observed quantities were diagonal in nature. Table 8 gives a typical set of standard deviations associated with the observed quantities.

Table 8

A Typical Set of Standard Deviations for Observed Quantities

	Observed Parameter	Standard Deviation ($\pm$)
Plate Coordinates	x_p (mm)	0.001
	y_p (mm)	0.001
Survey Coordinates	X_p (m)	1000
	Y_p (m)	1000
	Z_p (m)	1000
Principal Point Position	x_o (mm)	0.05
	y_o (mm)	0.05
Camera Station	X (m)	3
	Y (m)	3
	Z (m)	3

Table 8

(Continued)

	Observed Parameter	Standard Deviation (±)
Camera Attitude	κ (rad)	0.001
	ϕ (rad)	0.001
	ω (rad)	0.001
Camera Velocity	V_x (m/sec)	10
	V_y (m/sec)	10
	V_z (m/sec)	10
Camera Attitude Rates	$\dot{\kappa}$ (rad/sec)	0.01
	$\dot{\phi}$ (rad/sec)	0.01
	$\dot{\omega}$ (rad/sec)	0.01

In the example given in Table 8, the rotation elements are considered very well-known. However, tests run with these values relaxed yielded similar results. It should be noted that camera attitude in the Apollo J missions will be well-known from the coupled stellar camera.

As mentioned earlier, the most striking feature of these tests was the form of the resulting variance-covariance matrix of the adjusted quantities. The variances of the adjusted quantities were very similar to those used in the weighting matrices. This corres-

pondence between the variance-covariance matrix of the adjusted quantities and that associated with the observed quantities allows stability computations or estimates to be made prior to the solution of the system. The correct estimation of the precision of the observational process is therefore of great importance.

Consider the norm theory of Chapter 3 and in particular equation (3.18):

$$\|\delta X\|_\infty = \frac{\|A^{-1}\|_\infty \cdot \|E\|_\infty \cdot \|X\|_\infty + \|A^{-1}\|_\infty \cdot \|\delta Y\|_\infty}{1 - \|A^{-1}\|_\infty \cdot \|E\|_\infty} \qquad (3.18)$$

It is noted from Chapter 3 that $\|E\|_\infty = n.10^{-15}$ and that $\|\delta Y\|_\infty = 10^{-15}$ for the IRCC 360/75 in the double precision mode. Then $\|A^{-1}\|_\infty = \|N^{-1}\|_\infty$ and an upper limit for $\|N^{-1}\|_\infty$ can be estimated as $n.\max_i(\sigma_{ii})$ where σ_{ii} is the variance of an observation.

Similarly, $\|X\|_\infty = \|U\|_\infty = \max_i(u_i)$, hence the above equation becomes:

$$\|\delta X\|_{\infty \text{ upper limit}} = \frac{n.\max_i(\sigma_{ii}).n.10^{-15}.\max_i(u_i) + n.\max_i(\sigma_{ii}).10^{-15}}{1 - n.\max_i(\sigma_{ii}).n.10^{-15}}$$

which yields:

$$\|\delta X\|_{\infty \text{ upper limit}} = \frac{n^2.10^{-15}.\max_i(\sigma_{ii}).\max_i(u_i) + n.10^{-15}.\max_i(\sigma_{ii})}{1 - n^2.10^{-15}.\max_i(\sigma_{ii})}$$

In the tests associated with this chapter, the following conditions applied:

$$n = 100$$

$$\max_i(\tilde{\sigma}_{ii}) = 10^6$$

$$\max_i(u_i) = 10^8$$

Hence,

$$\|\delta X\|_{\infty \text{ upper limit}} = \frac{10^4 . 10^{-15} . 10^6 . 10^8 + 10^2 . 10^{-15} . 10^6}{1 - 10^4 . 10^{-15} . 10^6}$$

$$= \frac{10^3 + 10^{-7}}{1 - 10^{-5}} \approx 10^3$$

i.e. $$\|\delta X\|_{\infty \text{ upper limit}} \approx 10^3$$

This value applies to corrections to the survey coordinates and is of the same order as their estimated standard deviations, indicating that the adjustment procedure may not further improve known values.

An analysis of $\|\delta X\|_\infty$ after adjustment reduced its value to $\|\delta X\|_\infty \approx 10$, which indicates the level of significance of the solution to be approximately 1 part in 10^6. It should also be noted that row, column normalization was not performed on the normal equation matrix prior to inversion. This normalization should be done if the most representative norms are to be obtained.

In general, the procedure adopted required three iterations to converge to stable answers. The time for each iteration was 2 minutes 10 seconds for a total of twenty-four points. The greater

part of the time was spent in performing the analytical differentiation required for the partial differentials. One test was performed to compare the time required to determine the partial by numerical techniques. The following principles were applied:

Assume that $\frac{\partial F_1}{\partial \kappa}$ was required.

Then $$\frac{\partial F_1}{\partial \kappa} \approx \frac{(F_1)_{0+\delta} - (F)_0}{\delta}$$

where $(F_1)_0$ is F_1 evaluated for assumed values of the parameters.

$(F_1)_{0+\delta}$ is F_1 evaluated for the assumed values of the parameters with a small delta increment added to the differential parameter under investigation.

The numerical procedure was found to be an order of magnitude faster than the analytical differentiation and yielded the same numerical values. However the numerical agreement is dependent on the δ increment chosen. This concept requires further investigation as it was not feasible to continue this investigation.

In these block tests it was also noted that the coordinate values of the principal point did not seem to be as responsive to adjustment as they were in the single photo tests. This was in part overcome by using better estimates than had been initially contemplated. That is, the variance was decreased from 10^{-2} to 2.5×10^{-3} for observations on these parameters.

In the numerical tests, it was determined that a practical limit of 3 iterations was necessary for the moderately perturbed test data. As the perturbations became large, it was necessary to complete more iterations to achieve the same level of precision.

This level of precision, theoretically speaking, should have been extremely high, as it was assumed that $L_a = L_b$ for these tests. Hence, the residuals, V, are defined as $V = L_b - L_a = 0$. However, because of a number of factors, this will only be reached in the limit. The principal factors affecting this condition are as follows:

(a) The augmented collinearity condition equations are non-linear in nature. The susceptibility of these equations to this non-linearity was indicated in Section 4.241.

(b) The weights associated with the survey stations did not truly represent the situation, since no random errors were impressed upon these values. Thus, the convergence rate was slowed down due to this incorrect weight. Ideally, weights should accurately reflect the observational precision.

(c) The Y coordinate of the survey coordinate data appeared to lag behind both the X and Z coordinates in reaching the 10 meter residual level.

(d) The stability level of the solution was approximately 1 part in 10^6, hence unit accuracy in the adjusted survey positions is all that may be obtained.

Table 9 lists some typical values for tests associated with this section of the work. Since the precision of the adjusted

Table 9

Typical Values Associated with the n x m Photo Block with Fully Observed Parameters

	Parameter	True Value	Approximate Value	Corrections from first iteration
Parameters Associated with Photostation 1	x_o (mm)	0.200	0.200	0.0095
	y_o (mm)	0.225	0.240	-0.0149
	X_o (m)	4320000.	4319900.	108.1
	Y_o (m)	-200000.	-199990.	-19.8
	Z_o (m)	922000.	921900.	43.4
	ω (deg)	10.	9.9	0.10
	ϕ (deg)	80.	79.9	0.10
	κ (deg)	0.	0.0	0.
	V_x (m/sec)	100.	90.	10.0
	V_y (m/sec)	-100.	-95.	-5.0
	V_z (m/sec)	2000.	1995.	5.0
	$\dot{\omega}$ (^{o}/sec)	0.	0.	0.0
	$\dot{\phi}$ (^{o}/sec)	0.	0.	0.0
	$\dot{\kappa}$ (^{o}/sec)	0.	0.	0.0
Parameters Associated with Photostation 2	x_o (mm)	0.200	0.200	0.0045
	y_o (mm)	0.225	0.240	-0.0085
	X_o (m)	4320000.	4319900.	114.6
	Y_o (m)	200000.	199990.	-1.5
	Z_o (m)	922000.	921900.	69.9

Table 9

(Continued)

	Parameter	True Value	Approximate Value	Corrections from first iteration
Parameters Associated with Photostation 2	ω (deg)	10.	9.9	0.10
	ϕ (deg)	80.	79.9	0.10
	κ (deg)	0.	0.	0.0
	V_x (m/sec)	100.	90.	10.0
	V_y (m/sec)	100.	95.	5.0
	V_z (m/sec)	2000.	1995.	5.0
	$\dot{\omega}$ ($^\circ$/sec)	0.	0.	0.0
	$\dot{\phi}$ ($^\circ$/sec)	0.	0.	0.0
	$\dot{\kappa}$ ($^\circ$/sec)	0.	0.	0.0
Survey Station 1	X (m)	1731858.7	1731800.	61.6
	Y (m)	157282.2	157200.	46.9
	Z (m)	52983.5	52900.	29.4
Survey Station 2	X (m)	1696658.2	1696600.	40.2
	Y (m)	129022.7	129000.	0.3
	Z (m)	344260.9	344200.	63.4
Survey Station 3	X (m)	1726572.2	1726500.	58.3
	Y (m)	-106750.7	-106700.	-42.9
	Z (m)	192865.9	192800.	44.5

values after 3 iterations has already been mentioned, it was decided to present instead the corrections to be applied to the approximate values on completion of the first iteration. Thus the table illustrates, in a limited manner, the convergence characteristics of the solution.

5. SUMMARY

5.1 Conclusions

5.11 Principal Conclusions

The principal aim of the research presented in this report was to obtain, if possible, answers to those questions which were presented in the introductory section, Chapter 1.

However, before elaborating on the conclusions reached by the adoption of the model presented in Chapter 2, it is appropriate to mention briefly the pitfalls encountered in two abortive attempts to resolve the problems.

Preliminary attempts to correct for image motion by using Kawachi's[16] formulae were abandoned, as the expressions became unmanageable if the cause of image motion was not known. Work then continued with the aim of reducing this unmanageability by combining the individual corrections into a single uniform model, the existence of which had been intimated by Kawachi[16]. Unfortunately, this model could not be constructed. Consequently, the correction of image positions to a single uniform epoch corresponding to a central projection failed.

The second set of experiments involved some recently-published monomorphic relationships by Das[44]. These models included compensatory terms for focal plane shutters and image motion. However, a

large number of conditions exist under which the equations become singular. Testing of these equations indicated that these conditions would need to be completely understood before they could be successfully developed further.

In general, the collinearity condition equations do not exhibit singularity and, since they relate the object space to the image space, it was decided to augment these equations to handle a moving platform. The augmentation of the collinearity conditions with velocity and epoch of exposure does not alter the definition of the principal point which can be expressed as

> ... the point in a photograph or camera focal plane which is chosen as the centre of the image for relating the geometry of the image to the geometry of the object space. If the camera is distortion-free so that the geometry of the image is the same as that of a perspective projection of the object, then the principal point is the foot of the perpendicular to the image plane from the centre of projection.
>
> National Mapping Council of Australia[45]

Consequently, the position of the principal point remains as described, since the perspective geometry remains unaltered.

Image motion and image motion compensation do not alter the calibration of the interior orientation elements of the camera, of which the principal point is a component. However the resulting imagery may be deformed, such that the mathematical relationships between the image space and the object space are destroyed. In those instances when the product of exposure interval and image velocity is such that the expected blur is well below tolerable limits, the regular collinearity conditions can be used. However, for focal plane shutter systems where the travel time of the shut-

ter is considerably greater than the exposure interval, the augmented collinearity conditions should be used. In the event of the image motion being such that IMC needs to be applied, it is possible to correct the observed image coordinates. This correction is obtained by multiplying the exposure epoch, Δt, by the rate at which IMC was applied, then summing over the epochs.

With reference to the problem of incomplete calibration of the photographic system, it seems reasonable to expect that y_o, the unknown coordinate of the principal point, can be recovered dynamically from the block adjustment of the photographs. Recovery of this parameter is possible due to the unique nature of both the lunar surface and the photocoverage, resulting in very large variations in all three coordinates across the model. It is also due in part to the mathematical model used, especially the incorporation of observations on the elements of exterior orientation. However, there were also indications that the parameter recovered would be more exact if approximate values were first obtained by single photo space resection procedures.

5.12 Minor Conclusions

In addition to the solutions obtained for the main problem, a number of important features were observed during the work described above. They are as follows:

(a) The matrix norm theory appears to offer a stable method with upper bounds for determining the expected and actual precision of matrix solution methods. The conventional P, N or M numbers,

on the other hand, have no supremum. The matrix norm theory appears to offer "pre-inversion" insight for those situations where all parameters may be treated as observations; it also appears feasible to extend this theory to include other models.

(b) For large matrix systems, solution methods are faster and more stable than inverse methods. However, the variance-covariance matrix must be determined by secondary methods, such as the Monte Carlo method.

(c) Differentiation of complex analytical functions by numerical methods is very much faster than evaluation through their associated analytical expressions. The accuracy of such a process is dependent on the δ increment chosen for the evaluation process.

5.2 Recommendations

5.21 Recommendations Concerning Principal Conclusions

The principal conclusions were drawn, in part, from numerical tests using fictitious data. It is therefore recommended that a small real data test be performed so that the validity of the proposed model and the conclusions are confirmed. It is not recommended that a full triangulation with Lunar Orbiter photography be attempted, since photography using recovered imagery will shortly become available from the Apollo J missions. However, many of the ideas expressed in this report are directly applicable to the Apollo J missions and therefore warrant continued investigations.

5.22 Recommendations Concerning Minor Conclusions

It is recognised that the conclusions presented in Section 5.12 are based on insufficient data sets. There is, therefore, a need to increase the data base to ensure that the conclusions are justified. In addition, continued research should be conducted into the problems of stability and speed of execution, since the size of matrix systems in practical use continues to grow.

It is therefore strongly recommended that theoretical and practical research continue in the following areas:

(a) Stability indicators.

(b) Stable and efficient solution techniques.

(c) Economic formation of the necessary partials.

5.221 Recommendations on Stability Indicators

In view of the apparent success of the norm theory in indicating the stability characteristics of a fully-observed system, this approach should continue to receive attention so that stability indicators can be established for more general systems. In particular, investigations should be made into the possibility of establishing stability parameters for solutions obtained by non-inverse methods, such as the square root method of Section 3.6.

5.222 Recommendations on Stable and Efficient Solution Techniques

In Chapter 3, a number of techniques for the solution of large systems of equations were tested on the same large real system. Work of this nature must continue with all of the available algo-

rithms so that a complete understanding of the peculiarities of each algorithm can be obtained.

Recent developments in the discipline of Numerical Analysis indicate that it may soon be possible to accomplish much of this analysis by algebraic techniques, as well as by computational techniques.

Thus, with continued theoretical and practical work, an order for computational algorithms based on size of system, desired stability and economy may be established. This work must not be considered outside the scope of the Geodetic Scientist and left to the more abstract Mathematician.

5.223 Recommendations on the Economic Formation of Partials.

In this report, a single CPU time test was conducted on the efficiency of numerically evaluating the required partials. This test indicated that numerical evaluation could be achieved in 1/10 of the time required for analytical evaluation, without loss in accuracy. It is therefore recommended that the well-known block triangulation procedures using the collinearity conditions be rewritten using numerical evaluation of the partials, rather than analytical evaluations. The procedures are readily adaptable for different δ increments and, using the appropriate statistical methods, the quality of the resulting solution may be compared against that obtained through an analytical evaluation of the partials.

APPENDIX A

THE ROTATION MATRIX

The well-known rotation matrix has many variants. However the following form is common in Geodetic Science:

$$R = M = R_3 \, R_2 \, R_1 = R_\kappa \, R_\phi \, R_\omega$$

$$\text{i.e. } M = \begin{bmatrix} \cos\kappa & \sin\kappa & 0 \\ -\sin\kappa & \cos\kappa & 0 \\ 0 & 0 & 1 \end{bmatrix} \begin{bmatrix} \cos\phi & 0 & -\sin\phi \\ 0 & 1 & 0 \\ \sin\phi & 0 & \cos\phi \end{bmatrix} \begin{bmatrix} 1 & 0 & 0 \\ 0 & \cos\omega & \sin\omega \\ 0 & -\sin\omega & \cos\omega \end{bmatrix}$$

which yields on expansion:

$$M = \begin{bmatrix} \cos\phi\cos\kappa & \cos\omega\sin\kappa + \sin\omega\sin\phi\cos\kappa & \sin\omega\sin\kappa - \cos\omega\sin\phi\cos\kappa \\ -\cos\phi\sin\kappa & \cos\omega\cos\kappa - \sin\omega\sin\phi\sin\kappa & \sin\omega\cos\kappa + \cos\omega\sin\phi\sin\kappa \\ \sin\phi & -\sin\omega\cos\phi & \cos\omega\cos\phi \end{bmatrix}$$

It is now proposed to write the rotation matrix as a sum of two rotations $\alpha + \beta$

$$\text{i.e. } M = N = R_{(\kappa + \dot{\kappa}\Delta t)} \, R_{(\phi + \dot{\phi}\Delta t)} \, R_{(\omega + \dot{\omega}\Delta t)}$$

$$\text{i.e. } N = R_\kappa \, R_{\dot{\kappa}\Delta t} \, R_\phi \, R_{\dot{\phi}\Delta t} \, R_\omega \, R_{\dot{\omega}\Delta t}$$

Proof that $R_{(\alpha+\beta)} = R_\alpha R_\beta$

$$\text{Given that } R_\alpha = R_\kappa = \begin{bmatrix} \cos\kappa & \sin\kappa & 0 \\ -\sin\kappa & \cos\kappa & 0 \\ 0 & 0 & 1 \end{bmatrix}.$$

$$\text{and } R_\beta = R_{\dot\kappa\Delta t} = \begin{bmatrix} \cos \dot\kappa\Delta t & \sin \dot\kappa\Delta t & 0 \\ -\sin \dot\kappa\Delta t & \cos \dot\kappa\Delta t & 0 \\ 0 & 0 & 1 \end{bmatrix}$$

$$\text{then } R_\alpha R_\beta = \begin{bmatrix} \cos\kappa \cos \dot\kappa\Delta t & \cos\kappa \sin \dot\kappa\Delta t & 0 \\ -\sin\kappa \sin \dot\kappa\Delta t & +\sin\kappa \cos \dot\kappa\Delta t & \\ -\sin\kappa \cos \dot\kappa\Delta t & -\sin\kappa \sin \dot\kappa\Delta t & 0 \\ -\cos\kappa \sin \dot\kappa\Delta t & +\cos\kappa \cos \dot\kappa\Delta t & \\ 0 & 0 & 1 \end{bmatrix}$$

$$= \begin{bmatrix} \cos(\kappa + \dot\kappa\Delta t) & \sin(\kappa + \dot\kappa\Delta t) & 0 \\ -\sin(\kappa + \dot\kappa\Delta t) & \cos(\kappa + \dot\kappa\Delta t) & 0 \\ 0 & 0 & 1 \end{bmatrix}$$

$$= R_{(\kappa + \dot\kappa\Delta t)} = R_{(\alpha + \beta)}$$

Similarly, it can be proved that

$$R_\phi R_{\dot\phi\Delta t} = R_{(\phi + \dot\phi\Delta t)}$$

and

$$R_\omega R_{\dot\omega\Delta t} = R_{(\omega + \dot\omega\Delta t)}$$

Hence, N may be written explicitly in the form given on the following page, from which it is evident that the concept of N is analagous to that of the general rotation matrix M.

$$
\begin{bmatrix}
\cos(\phi+\dot{\phi}\Delta t)\cos(\kappa+\dot{\kappa}\Delta t) & \cos(\omega+\dot{\omega}\Delta t)\sin(\kappa+\dot{\kappa}\Delta t) & \sin(\omega+\dot{\omega}\Delta t)\sin(\kappa+\dot{\kappa}\Delta t) \\
 & +\sin(\omega+\dot{\omega}\Delta t)\sin(\phi+\dot{\phi}\Delta t)\cos(\kappa+\dot{\kappa}\Delta t) & -\cos(\omega+\dot{\omega}\Delta t)\sin(\phi+\dot{\phi}\Delta t)\cos(\kappa+\dot{\kappa}\Delta t) \\
-\cos(\phi+\dot{\phi}\Delta t)\sin(\kappa+\dot{\kappa}\Delta t) & \cos(\omega+\dot{\omega}\Delta t)\cos(\kappa+\dot{\kappa}\Delta t) & \sin(\omega+\dot{\omega}\Delta t)\cos(\kappa+\dot{\kappa}\Delta t) \\
 & -\sin(\omega+\dot{\omega}\Delta t)\sin(\phi+\dot{\phi}\Delta t)\sin(\kappa+\dot{\kappa}\Delta t) & +\cos(\omega+\dot{\omega}\Delta t)\sin(\phi+\dot{\phi}\Delta t)\sin(\kappa+\dot{\kappa}\Delta t) \\
\sin(\phi+\dot{\phi}\Delta t) & -\sin(\omega+\dot{\omega}\Delta t)\cos(\phi+\dot{\phi}\Delta t) & \cos(\omega+\dot{\omega}\Delta t)\cos(\phi+\dot{\phi}\Delta t)
\end{bmatrix}
$$

The rotation matrix can be differentiated readily either from the basic elemental rules or via skew symmetric matrices, P_α. Computationally, the elemental method is superior to the skew symmetric method. However, algebraically the skew symmetric idea has many advantages (see Lucas[46]).

The following definitions should be noted for differentiation by skew symmetric matrices:

$$\frac{dR_3}{d\alpha} = \frac{\partial}{\partial\alpha} \cdot P_3R_3 = \frac{\partial}{\partial\alpha} R_3P_3$$

$$\frac{dR_2}{d\alpha} = \frac{\partial}{\partial\alpha} \cdot P_2R_2 = \frac{\partial}{\partial\alpha} R_2P_2$$

$$\frac{dR_1}{d\alpha} = \frac{\partial}{\partial\alpha} \cdot P_1R_1 = \frac{\partial}{\partial\alpha} R_1P_1$$

Hence, using skew symmetric matrices, the $\dot{N}$ matrix can be expressed as:

$$\dot{N} = \frac{\partial}{\partial\Delta t} P_3R_3R_2R_1 + R_3 \frac{\partial}{\partial\Delta t} P_2R_2R_1 + R_3R_2 \frac{\partial}{\partial\Delta t} R_1P_1$$

$$= \dot{\kappa}P_3R_3R_2R_1 + \dot{\phi}R_3P_2R_2R_1 + \dot{\omega}R_3R_2R_1P_1$$

Table 10 lists the matrix components necessary to evaluate $\dot{N}$ by the skew symmetric method. The elemental expansion of $\dot{N}$ is given on page 97.

Table 10

Some Principal Components of the Matrices N and $\dot{N}$

α	R_α	$R_{\dot{\alpha}\Delta t}$	$\frac{\partial R_{\dot{\alpha}\Delta t}}{\partial \Delta t}$	P_α
3	$\begin{bmatrix} \cos\kappa & \sin\kappa & 0 \\ -\sin\kappa & \cos\kappa & 0 \\ 0 & 0 & 1 \end{bmatrix}$	$\begin{bmatrix} \cos(\dot{\kappa}\Delta t) & \sin(\dot{\kappa}\Delta t) & 0 \\ -\sin(\dot{\kappa}\Delta t) & \cos(\dot{\kappa}\Delta t) & 0 \\ 0 & 0 & 1 \end{bmatrix}$	$\begin{bmatrix} -\dot{\kappa}\sin(\dot{\kappa}\Delta t) & \dot{\kappa}\cos(\dot{\kappa}\Delta t) & 0 \\ -\dot{\kappa}\cos(\dot{\kappa}\Delta t) & -\dot{\kappa}\sin(\dot{\kappa}\Delta t) & 0 \\ 0 & 0 & 0 \end{bmatrix}$	$\begin{bmatrix} 0 & 1 & 0 \\ -1 & 0 & 0 \\ 0 & 0 & 0 \end{bmatrix}$
2	$\begin{bmatrix} \cos\phi & 0 & -\sin\phi \\ 0 & 1 & 0 \\ \sin\phi & 0 & \cos\phi \end{bmatrix}$	$\begin{bmatrix} \cos(\dot{\phi}\Delta t) & 0 & -\sin(\dot{\phi}\Delta t) \\ 0 & 1 & 0 \\ \sin(\dot{\phi}\Delta t) & 0 & \cos(\dot{\phi}\Delta t) \end{bmatrix}$	$\begin{bmatrix} -\dot{\phi}\sin(\dot{\phi}\Delta t) & 0 & -\dot{\phi}\cos(\dot{\phi}\Delta t) \\ 0 & 0 & 0 \\ \dot{\phi}\cos(\dot{\phi}\Delta t) & 0 & -\dot{\phi}\sin(\dot{\phi}\Delta t) \end{bmatrix}$	$\begin{bmatrix} 0 & 0 & -1 \\ 0 & 0 & 0 \\ 1 & 0 & 0 \end{bmatrix}$
1	$\begin{bmatrix} 1 & 0 & 0 \\ 0 & \cos\omega & \sin\omega \\ 0 & -\sin\omega & \cos\omega \end{bmatrix}$	$\begin{bmatrix} 1 & 0 & 0 \\ 0 & \cos(\dot{\omega}\Delta t) & \sin(\dot{\omega}\Delta t) \\ 0 & -\sin(\dot{\omega}\Delta t) & \cos(\dot{\omega}\Delta t) \end{bmatrix}$	$\begin{bmatrix} 0 & 0 & 0 \\ 0 & -\dot{\omega}\sin(\dot{\omega}\Delta t) & \dot{\omega}\cos(\dot{\omega}\Delta t) \\ 0 & \dot{\omega}\cos(\dot{\omega}\Delta t) & -\dot{\omega}\sin(\dot{\omega}\Delta t) \end{bmatrix}$	$\begin{bmatrix} 0 & 0 & 0 \\ 0 & 0 & 1 \\ 0 & -1 & 0 \end{bmatrix}$

The $\dot{N}$ Matrix

$$
\begin{bmatrix}
-\dot{\phi}\sin(\phi+\dot{\phi}\Delta t)\cos(\kappa+\dot{\kappa}\Delta t) & -\dot{\omega}\sin(\omega+\dot{\omega}\Delta t)\sin(\kappa+\dot{\kappa}\Delta t) & \dot{\omega}\cos(\omega+\dot{\omega}\Delta t)\sin(\kappa+\dot{\kappa}\Delta t) \\
-\dot{\kappa}\cos(\phi+\dot{\phi}\Delta t)\sin(\kappa+\dot{\kappa}\Delta t) & +\dot{\kappa}\cos(\omega+\dot{\omega}\Delta t)\cos(\kappa+\dot{\kappa}\Delta t) & +\dot{\kappa}\sin(\omega+\dot{\omega}\Delta t)\cos(\kappa+\dot{\kappa}\Delta t) \\
 & +\dot{\omega}\cos(\omega+\dot{\omega}\Delta t)\sin(\phi+\dot{\phi}\Delta t)\cos(\kappa+\dot{\kappa}\Delta t) & +\dot{\omega}\sin(\omega+\dot{\omega}\Delta t)\sin(\phi+\dot{\phi}\Delta t)\cos(\kappa+\dot{\kappa}\Delta t) \\
 & +\dot{\phi}\sin(\omega+\dot{\omega}\Delta t)\cos(\phi+\dot{\phi}\Delta t)\cos(\kappa+\dot{\kappa}\Delta t) & -\dot{\phi}\cos(\omega+\dot{\omega}\Delta t)\cos(\phi+\dot{\phi}\Delta t)\cos(\kappa+\dot{\kappa}\Delta t) \\
 & -\dot{\kappa}\sin(\omega+\dot{\omega}\Delta t)\sin(\phi+\dot{\phi}\Delta t)\sin(\kappa+\dot{\kappa}\Delta t) & +\dot{\kappa}\cos(\omega+\dot{\omega}\Delta t)\sin(\phi+\dot{\phi}\Delta t)\sin(\kappa+\dot{\kappa}\Delta t) \\
 & & \\
\dot{\phi}\sin(\phi+\dot{\phi}\Delta t)\sin(\kappa+\dot{\kappa}\Delta t) & -\dot{\omega}\sin(\omega+\dot{\omega}\Delta t)\cos(\kappa+\dot{\kappa}\Delta t) & \dot{\omega}\cos(\omega+\dot{\omega}\Delta t)\cos(\kappa+\dot{\kappa}\Delta t) \\
+\dot{\kappa}\cos(\phi+\dot{\phi}\Delta t)\cos(\kappa+\dot{\kappa}\Delta t) & -\dot{\kappa}\cos(\omega+\dot{\omega}\Delta t)\sin(\kappa+\dot{\kappa}\Delta t) & -\dot{\kappa}\sin(\omega+\dot{\omega}\Delta t)\sin(\kappa+\dot{\kappa}\Delta t) \\
 & -\dot{\omega}\cos(\omega+\dot{\omega}\Delta t)\sin(\phi+\dot{\phi}\Delta t)\sin(\kappa+\dot{\kappa}\Delta t) & -\dot{\omega}\sin(\omega+\dot{\omega}\Delta t)\sin(\phi+\dot{\phi}\Delta t)\sin(\kappa+\dot{\kappa}\Delta t) \\
 & -\dot{\phi}\sin(\omega+\dot{\omega}\Delta t)\cos(\phi+\dot{\phi}\Delta t)\sin(\kappa+\dot{\kappa}\Delta t) & +\dot{\phi}\cos(\omega+\dot{\omega}\Delta t)\cos(\phi+\dot{\phi}\Delta t)\sin(\kappa+\dot{\kappa}\Delta t) \\
 & -\dot{\kappa}\sin(\omega+\dot{\omega}\Delta t)\sin(\phi+\dot{\phi}\Delta t)\cos(\kappa+\dot{\kappa}\Delta t) & +\dot{\kappa}\cos(\omega+\dot{\omega}\Delta t)\sin(\phi+\dot{\phi}\Delta t)\cos(\kappa+\dot{\kappa}\Delta t) \\
 & & \\
\dot{\phi}\cos(\phi+\dot{\phi}\Delta t) & -\dot{\omega}\cos(\omega+\dot{\omega}\Delta t)\cos(\phi+\dot{\phi}\Delta t) & -\dot{\omega}\sin(\omega+\dot{\omega}\Delta t)\cos(\phi+\dot{\phi}\Delta t) \\
 & +\dot{\phi}\sin(\omega+\dot{\omega}\Delta t)\sin(\phi+\dot{\phi}\Delta t) & -\dot{\phi}\cos(\omega+\dot{\omega}\Delta t)\sin(\phi+\dot{\phi}\Delta t)
\end{bmatrix}
$$

APPENDIX B

TWO DECOMPOSITION EXAMPLES

The decomposition of equation set (2.6) to the specific forms of Kawachi[14,15] is illustrated by the following two cases.

Case 1: Vertical photography, translation along flight direction only

The following conditions apply:

$\kappa = \phi = \omega = 0 \quad \therefore \; N = I$

$\dot{\kappa} = \dot{\phi} = \dot{\omega} = 0 \quad \therefore \; \dot{N} = I$

$$V = \begin{bmatrix} V_x \\ 0 \\ 0 \end{bmatrix}$$

$\Delta t = 0$

$$\text{then } \dot{x}_p = -f\left\{\left\{\left\{\begin{bmatrix}1 & 0 & 0\end{bmatrix}\left(\begin{bmatrix}X\\Y\\Z\end{bmatrix}_p - \begin{bmatrix}X\\Y\\Z\end{bmatrix}_o - \begin{bmatrix}V_x\\0\\0\end{bmatrix}\cdot 0\right) - \begin{bmatrix}1 & 0 & 0\end{bmatrix}\begin{bmatrix}V_x\\0\\0\end{bmatrix}\right\}\cdot \right.\right.$$

$$\left.\left\{\begin{bmatrix}0 & 0 & 1\end{bmatrix}\left(\begin{bmatrix}X\\Y\\Z\end{bmatrix}_p - \begin{bmatrix}X\\Y\\Z\end{bmatrix}_o - \begin{bmatrix}V_x\\0\\0\end{bmatrix}\cdot 0\right)\right\}\right\} -$$

$$\left\{\left\{\begin{bmatrix}0 & 0 & 1\end{bmatrix}\left(\begin{bmatrix}X\\Y\\Z\end{bmatrix}_p - \begin{bmatrix}X\\Y\\Z\end{bmatrix}_o - \begin{bmatrix}V_x\\0\\0\end{bmatrix}\cdot 0\right) - \begin{bmatrix}0 & 0 & 1\end{bmatrix}\begin{bmatrix}V_x\\0\\0\end{bmatrix}\right\}\cdot\right.$$

$$\left\{\left[1\ 0\ 0\right]\left(\begin{bmatrix}X\\Y\\Z\end{bmatrix}_p - \begin{bmatrix}X\\Y\\Z\end{bmatrix}_o - \begin{bmatrix}V_x\\0\\0\end{bmatrix}\cdot o\right)\right\}\cdot$$

$$\left\{\left[0\ 0\ 1\right]\left(\begin{bmatrix}X\\Y\\Z\end{bmatrix}_p - \begin{bmatrix}X\\Y\\Z\end{bmatrix}_o - \begin{bmatrix}V_x\\0\\0\end{bmatrix}\cdot o\right)\right\}^{-2}$$

$$\text{Hence } \dot{x}_p = \frac{-f\cdot\left[(X_p - X_o - V_x)\cdot(Z_p - Z_o) - (Z_p - Z_o)\cdot(X_p - X_o)\right]}{(Z_p - Z_o)^2}$$

$$= \frac{f\cdot V_x\cdot(Z_p - Z_o)}{(Z_p - Z_o)^2} = \frac{f\cdot V_x}{(Z_p - Z_o)} = \frac{-f\cdot V_x}{h}$$

The minus sign is a result of the equations being formulated for the diapositive position with elevation up.

cf. Kawachi: $\dot{x}_p = \frac{Vf}{h}$, h being defined as modulus h.

It is obvious that $\dot{y}_p = 0$ since $N_2 = \dot{N}_2 = \left[0\ 1\ 0\right]$, hence the numerator of the function equals zero.

Case 2: <u>Vertical photography, platform pitching ($\dot{\phi}$)</u>

The following conditions apply:

$\kappa = \phi = \omega = 0 \quad \therefore N = I$

$\dot{\kappa} = \dot{\omega} = 0$

$\dot{\phi} \neq 0$

$V = 0$

$\Delta t = 0$

$$\text{then } \dot{x}_p = -f\left\{\left\{\left\{\left\{\begin{bmatrix}0 & 0 & \dot{n}_{13}\end{bmatrix}\left(\begin{bmatrix}X\\Y\\Z\end{bmatrix}_p - \begin{bmatrix}X\\Y\\Z\end{bmatrix}_o - 0\right) - \begin{bmatrix}1 & 0 & 0\end{bmatrix}\cdot 0\right\}\cdot \left\{\begin{bmatrix}0 & 0 & 1\end{bmatrix}\left(\begin{bmatrix}X\\Y\\Z\end{bmatrix}_p - \begin{bmatrix}X\\Y\\Z\end{bmatrix}_o - 0\right)\right\}\right\} - \left\{\left\{\begin{bmatrix}\dot{n}_{31} & 0 & 0\end{bmatrix}\left(\begin{bmatrix}X\\Y\\Z\end{bmatrix}_p - \begin{bmatrix}X\\Y\\Z\end{bmatrix}_o - 0\right) - \begin{bmatrix}0 & 0 & 1\end{bmatrix}\cdot 0\right\}\cdot \left\{\begin{bmatrix}1 & 0 & 0\end{bmatrix}\left(\begin{bmatrix}X\\Y\\Z\end{bmatrix}_p - \begin{bmatrix}X\\Y\\Z\end{bmatrix}_o - 0\right)\right\}\right\}\cdot \left\{\begin{bmatrix}0 & 0 & 1\end{bmatrix}\left(\begin{bmatrix}X\\Y\\Z\end{bmatrix}_p - \begin{bmatrix}X\\Y\\Z\end{bmatrix}_o - 0\right)\right\}^{-2}$$

Now $\dot{n}_{13} = -\dot{\phi}$ and $\dot{n}_{31} = \dot{\phi}$ from Appendix D.

Hence

$$\dot{x}_p = \frac{-f\left[-\dot{\phi}(Z_p - Z_o) \cdot (Z_p - Z_o) - \dot{\phi}(X_p - X_o) \cdot (X_p - X_o)\right]}{(Z_p - Z_o)^2}$$

$$= f\left[(Z_p - Z_o) \cdot (Z_p - Z_o) + (X_p - Z_o)^2\right]\frac{\dot{\phi}}{(Z_p - Z_o)^2}$$

$$= f\left[1 + \frac{(X_p - X_o)^2}{(Z_p - Z_o)^2}\right]\dot{\phi}$$

Now for vertical photography $\left|\frac{X_p - X_o}{Z_p - Z_o}\right| = \left|\frac{x_p - x_o}{f}\right|$ by virtue of similar triangles.

Hence $\dot{x}_p = \left[\frac{f^2 + (x_p - x_o)^2}{f}\right]\dot{\phi}$

cf. Kawachi: $\dot{x}_p = \left[\frac{f^2 + x^2}{f}\right]\dot{\phi}$

The y image velocity can be treated in a similar fashion.

APPENDIX C

MATRIX NORMS

It is required to prove the following three identities of Section 3.1.

(a) Proof that $(I + C)$ is non-singular if $\|C\| < 1$.

Consider the eigenvalue equation $CX = \lambda X$.

Applying the rules stated in Chapter 3 to each side of the eigenvalue equation

$$\|CX\| \leq \|C\| \cdot \|X\| \quad \text{and} \quad \|\lambda X\| = |\lambda| \cdot \|X\|$$

Hence, $\lambda_i < \|C\|$

Now, $(I + C)$ non-singular implies

$$(I + C) = \prod_{i}^{i=n} (1 + \lambda_i) \neq 0$$

where λ_i is the eigenvalue of matrix C

and if $|\lambda_i| < \|C\| < 1$, then λ_i must lie between $-1 + \epsilon$ and $1 - \epsilon$, where ϵ is a small quantity. Hence, $\prod_{i}^{i=n} (1 + \lambda_i) \neq 0$, which implies $|(I + C)| \neq 0$, and therefore the statement $|\lambda_i| < \|C\| < 1$ is true.

Using the previously stated identities, it is now useful to derive an inequality for the matrix $C = A - B$.

Consider $\|A\| = \|A - B + B\| \leq \|A - B\| + \|B\|$

Then $\|A\| - \|B\| \leq \|A - B\|$

or $\|A - B\| \geq \|A\| - \|B\|$

Moreover, $\|A - B\| = \|B - A\| \geq \|B\| - \|A\|$

and so $\|B - A\| \geq \|A\| - \|B\|$

(b) Proof $\|(I + C)^{-1}\| \leq \dfrac{1}{1 - \|C\|}$

Let $G = (I + C)^{-1}$

Then $(I + C) \cdot G = I$ or $I = G - (-1)CG$

Taking norms in the prescribed manner,

$$\|I\| = \|G - (-1)CG\|$$
$$1 \geq \|G\| - \|(-1)CG\|$$
$$1 \geq \|G\| - \|C\| \cdot \|G\|$$
$$1 \geq \|G\| \cdot \left[1 - \|C\|\right]$$

and hence $\|G\| = \|(I + C)^{-1}\| \leq \dfrac{1}{1 - \|C\|}$ QED

(c) Proof $\|I - (I + C)^{-1}\| = \dfrac{\|C\|}{1 - \|C\|}$

Let $G = I - (I + C)^{-1}$

Then $(I + C) \cdot G = G + CG = G - (-1)CG$

and $(I + C) \cdot (I - (I + C)^{-1}) = (I + C) - I = C$

Hence $C = G - (-1)CG$

Taking norms of both sides as prescribed,

$$\|C\| \geq \|G\| - \|(-1)CG\|$$
$$\geq \|G\| - \|CG\|$$
$$\geq \|G\| \cdot \left[1 - \|C\|\right]$$

and hence $\|G\| = \|I - (I + C)^{-1}\| \leq \dfrac{\|C\|}{1 - \|C\|}$ QED

APPENDIX D

AN EXAMPLE OF A TRIDIAGONAL FORM IN GEODETIC SCIENCE

Consider the following difference network where station 0 is known:

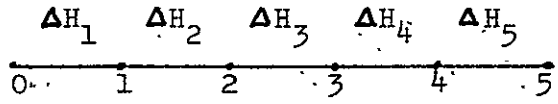

Then the solution is given by $-(A^TPA)^{-1}APL$, Uotila[24].

Assuming $P = I$, then

$$A = \begin{bmatrix} 1 & 0 & 0 & 0 & 0 \\ -1 & 1 & 0 & 0 & 0 \\ 0 & -1 & 1 & 0 & 0 \\ 0 & 0 & -1 & 1 & 0 \\ 0 & 0 & 0 & -1 & 1 \end{bmatrix}$$

$$A^T = \begin{bmatrix} 1 & -1 & 0 & 0 & 0 \\ 0 & 1 & -1 & 0 & 0 \\ 0 & 0 & 1 & -1 & 0 \\ 0 & 0 & 0 & 1 & -1 \\ 0 & 0 & 0 & 0 & 1 \end{bmatrix} \begin{bmatrix} 2 & -1 & 0 & 0 & 0 \\ -1 & 2 & -1 & 0 & 0 \\ 0 & -1 & 2 & -1 & 0 \\ 0 & 0 & -1 & 2 & -1 \\ 0 & 0 & 0 & -1 & 1 \end{bmatrix} = (A^TIA) \text{ which is tridiagonal}$$

APPENDIX E

REFERENCED COMPUTER PROGRAMS

(FORTRAN IV)

```
C*******************************************************************************
C
C     THE REINFORCEMENT METHOD OF INVERTING A MATRIX BY P.MORGAN JULY 1970
C
C     THIS IS A METHOD OF INVERTING LARGE MATRICES OUTSIDE THE CORE REGION.
C     THE DIRECT ACCESS FACILITY IS INVOKED TO HOLD THE NORMAL EQUATION
C     MATRIX AND ITS INVERSE.
C     REFERENCE  FACDEEV AND FACDEEVA PP 173
C     THIS  SUBROUTINE IS NOT UNIVERSAL WITHOUT CHANGES TO THE NECESSARY
C     INTEGER CONSTANTS.THIS COULD BE CHANGED IF PARAMETER TRANSMISSION
C     VIA THE CALLING SEQUENCE WAS ACCEPTABLE TO THE USER.
C     UNIT 3 IS ASSUMED TO HAVE THE NORMALS WHILE UNIT 4 WILL HAVE INVERSE
C     THE SUBROUTINE HAS NO CALLING PARAMETERS AND DATA TRANSMISSION,WHERE
C     NECESSARY IS UNDER A VARIABLE FORMAT, DOUBLE PRECISION IS USED.
C     ALL STATEMENTS PROCEEDED BY A  C/*/ CARD MUST BE MODIFIED TO SUIT JOB.
C     N IS ORDER OF MATRIX .THIS GOVERNS THE NUMBER OF RECORDS IN THE FILE
C     THERE BEING ONE RECORD PER ROW.
C
C*******************************************************************************
C
      SUBROUTINE  LINVRT
      IMPLICIT REAL *8 (A-H,O-Z)
C/*/
      DIMENSION A(75),V(75),B(75),RHO(75),BS(75),W(75)
C/*/  THE NUMBER OF ROWS AND/OR COLUMNS OF NORMALS IS DEFINED
      N=75
      CALL SCLOK1
C/*/  THE FILES ARE DEFINED
      DEFINE FILE 3(75,150,U,NN),4(75,150,U,NN)
C
C     LOAD FILE 4 WITH A UNIT MATRIX
C
      DO 11 I=1,N
      DO 12 I2=1,N
      A(I2) =0.D0
   12 CONTINUE
      A(I)  =1.D0
      WRITE(4'I) (A(I4),I4=1,N)
      READ(3'I)(A(I4),I4=1,N)
      IF(I.LT.N) FIND (3'I+1)
      W(I)=A(I)
       DO 13 I4=1,N
   13 A(I4)=A(I4)/W(I)
      WRITE(3'I) (A(I4),I4=1,N)
   11 CONTINUE
      DO 50 I10 = 1,N
      READ(3'I10,ERR=1000) (V(I11),I11=1,N)
      IF(I10.LT.N) FIND (3'I10+1 )
      V(I10) =0.D0
      DO 55 I15 = 1,N
```

```
      RHC(I15)  = 0.D0
      DO 51 I12 = 1,N
      READ(4'I12,ERR=1001) (A(I13),I13=1,N)
      IF(I12.LT.N)  FIND (4'I12+1)
      B(I12) = A(I15)
   51 CONTINUE
      IF(I10.NE.I15) GO TO 45
      DO 46 I12 =1,N
      BS(I12) = B(I12)
   46 CONTINUE
   45 DO 52 I12 =1,N
      RHC(I15) =RHC(I15) +B(I12)* V(I12)
   52 CONTINUE
   55 CONTINUE
      RHOKP1 = RHO(I10) + 1.D0
      DO 53  I17 =1,N
      RHC(I17)= RHC(I17)/ RHOKP1
   53 CONTINUE
      DO 60 I20 =1,I10
      READ(4'I20,ERR=1002) (A(I18),I18=1,N)
      IF(I20.LT.I10)  FIND (4'I20+1 )
      DO 61 I21 =1,N
      A(I21) = A(I21) - RHO(I21)*BS(I20)
   61 CONTINUE
      WRITE(4'I20)              (A(I18),I18=1,N)
   60 CONTINUE
      TIME=(RCLOK1(1.))/60.0
      WRITE(6,998) I10,TIME
   50 CONTINUE
      DO 14 I=1,N
      READ(3'I) (A(I15),I15=1,N)
      IF (I.LT.N) FIND (3'I+1)
      DO 15 I15=1,N
   15 A(I15)=A(I15)*W(I)
      WRITE(3'I) (A(I15),I15=1,N)
       READ(4'I) (A(I15),I15=1,N)
      IF(I.LT.N) FIND (4'I+1)
      DO 16 I15=1,N
   16 A(I15)=A(I15)/W(I15)
      WRITE(4'I) (A(I15),I15=1,N)
   14 CONTINUE
      WRITE(6,999)
      RETURN
 1000 WRITE(6,1010)
      CALL EXIT
 1001 WRITE(6,1011)
      CALL EXIT
 1002 WRITE(6,1012)
      CALL EXIT
  998 FORMAT (1X,'TUPLE NUMBER ',I3,' NOW EXECUTED. TOTAL EXECUTION TIME
```

```
     1 ELAPSED IN MINUTES IS ',F10.3 )
  999 FORMAT (1H1,5X,'NORMAL EXIT FROM LINVRT ACCOMPLISHED ' )
 1010 FORMAT(1X,'PROGRAMMERS ERROR MESSAGE: ERROR IN READING DIRECT ACCE
     1SS DEVICE FOR V MATRIX.EXECUTION TERMINATED.**********************'
     2/,1X,120(1H*),/)
 1011 FORMAT(1X,'PROGRAMMERS ERROR MESSAGE: ERROR IN READING DIRECT ACCE
     1SS DEVICE FOR A MATRIX USED TO FORM B MATRIX.EXECUTION TERMINATED'
     2/,1X,120(1H*),/)
 1012 FORMAT(1X,'PROGRAMMERS ERROR MESSAGE: ERROR IN READING DIRECT ACCE
     1SS DEVICE FOR A MATRIX USED TO ADD CORRECTIONS TO.EXECUTION TERMI'
     2/ ,1X,'-NATED.',114(1H*),/)
      RETURN
      END
```

```
C
C*******************************************************************************
C
C     MATRIX INVERSE BY REFINEMENT.P.MORGAN SEPTEMBER 1970
C
C     THIS IS A DOUBLE PRECISION SUBROUTINE WITH 2 ENTRY POINTS FOR REFINING
C     THE INVERSE OF A GIVEN MATRIX AND ITS INVERSE.
C     THE MAIN JCL MUST PROVIDE TWO DISK WORK SPACES:UNITS 1 AND 2 . THESE
C     WORK SPACES SHOULD BE SUCH THAT THE RECORD LENGTH EQUALS THE LENGTH
C     OF A ROW. ALL DATA TRANSMISSION IS ACCORDING TO THE VARIABLE FORMAT
C     RULES.
C     DISK UNITS 3 AND 4 HOLD THE GIVEN MATRIX AND ITS INVERSE ACCORDING TO
C     RULES ESTABLISHED FOR THE WORK SPACES.
C     N IS ORDER OF MATRIX
C     MAX IS MAXIMUM NUMBER OF ITTERATIONS
C     ACC IS ACCURACY LEVEL
C     MRET IS A RETURN MESSAGE CODE: 0,1,2
C
C*******************************************************************************
C
      SUBROUTINE  REFINE( N,MAX,ACC,MRET,NOP)
C     THIS ENTRY POINT ALLOWS LOOPING WITHIN THE SUBROUTINE. DETAILED OUTPUT
C     AFTER EACH STAGE OF THE COMPUTATIONS.
C     NOTE:IF NOP=1 THE PROGRAM SWITCHES TO EFFICIENT VERSION OF SUBROUTINE
      IMPLICIT REAL *8  (A-H,O-Z)
      DIMENSION A(5),B(5),C(5),G(5)
      REWIND 1
      REWIND 2
      REWIND 3
      REWIND 4
      IREP = 0
       IF (NOP.EQ.1) GO TO 716
    2 REWIND 4
      READ (4) B
      REWIND 4
      BB = B(1)
      NCOUNT = 0
    1 NCOUNT = NCOUNT + 1
      DO 11 I=1,N
      READ (3)  A
      DO 12 I1 =1,N
      READ (4) B
      C(I1)=0.D0
      DO 13 I2 =1,N
      C(I1) = C(I1)+A(I2)*B(I2)
   13 CONTINUE
   12 CONTINUE
      REWIND 4
      WRITE(2) C
   11 CONTINUE
```

```
      REWIND 2
      REWIND 3
      REWIND 4
      WRITE(6,701)
701   FORMAT (1H1,'PRODUCT AD',//)
      DO 700 I=1,N
      WRITE(6,101) I
      READ (2) C
700   WRITE(6,102) C
      REWIND 2
      DO 15 I=1,N
      READ (2) C
      DO 16 I1=1,N
      C(I1) = - C(I1)
 16   CONTINUE
      C(I)  = C(I)+1.DO
      WRITE(1) C
 15   CONTINUE
       REWIND 1
      REWIND 2
      DO 17 I=1,N
      READ (1) C
      WRITE (2) C
      WRITE(8) C
 17   CONTINUE
      REWIND 1
      REWIND 2
      REWIND 8
      WRITE(6,705)
705   FORMAT (1H1,'UNIT MATRIX - AD ',//)
      DO 706 I=1,N
      WRITE(6,101) I
      READ (2) C
706   WRITE(6,102) C
      REWIND 2
      DO 21 I=1,N
      READ (4) B
      DO 22 I1=1,N
      C(I1)=0.DO
      DO 26 I2=1,N
      READ (2) C
 26   A(I2)=C(I1)
      REWIND 2
      DO 23 I2=1,N
 23   C(I1)=C(I1)+B(I2)*A(I2)
 22   CONTINUE
      WRITE (1) C
 21   CONTINUE
      REWIND 1
      REWIND 2
```

```
      REWIND 3
      REWIND 4
      WRITE(6,709)
  709 FORMAT (1HI,'D*(I-AD)  ').
      DO 710 I=1,N
      WRITE(6,101) I
      READ (1) C
  710 WRITE(6,102) C
      REWIND 1
      DO 30 I=1,N
      READ (1) C
      READ (4) B
      DO 31 I1= 1,N
      B(I1) =B(I1)+C(I1)
   31 CONTINUE
      WRITE(2) B
   30 CONTINUE
      REWIND 1
      REWIND 2
      REWIND 4
      DO 32 I=1,N
      READ (2) C
      WRITE(4) C
   32 CONTINUE
      REWIND 1
      REWIND 2
      REWIND 4
C     A REFINEMENT HAS NOW BEEN ACCOMPLISHED
C     WRITE OUT  THE INVERSE
      WRITE (6,100) NCOUNT
      DO 35 I = 1,N
      WRITE (6,101) I
      READ (4) B
      WRITE(6,102 ) (B(I1),I1=1,N)
   35 CONTINUE
      REWIND 4
      IF(NCOUNT.GT.MAX) GO TO 36
      READ (4) B
      BBI = B(1)
      REWIND 4
      IF ( DABS(BB-BBI).LT. DABS(BB*5.0-14)) GO TO 36
      BB  = BBI
      GO TO  1
   36 DO 40 I =1,N
      D(I) = 0.00
       READ (8) A
      DO 41 I1=1,N
      D(I)  = C(I) + DABS(A(I1))
   41 CONTINUE
   40 CONTINUE
```

```
      REWIND 8
      AMAX = C(1)
      DO 42 I =1,N
      IF ( AMAX.LT.C(I)) AMAX= C(I)
   42 CONTINUE
      DO 43 I=1,N
      C(I) = 0.DO
      READ (4) A
      DO 44 II=1,N
      C(I) = C(I) + CABS(A(II))
   44 CONTINUE
   43 CONTINUE
      BMAX = C(1)
      DO 45 I=1,N
      IF ( BMAX.LT.C(I)) BMAX= C(I)
   45 CONTINUE
      ACCUR  =   BMAX* AMAX*AMAX/(1.DO-AMAX)
      IF ( AMAX .GT. 1.DO ) GO TO 600
      IF ( ACCUR.GT. ACC  ) GO TO 601
      WRITE(6,107) NCOUNT, ACCUR
      MRET = 0
      RETURN
  601 WRITE(6,104) MAX,ACCUR,ACC
      IREP  =IREP+1
      IF(IREP.GE.2) GO TO 603
      WRITE(6,105)
      GO TO    2
  603 WRITE(6,106)
      MRET    = 2
      RETURN
  600 WRITE(6,103)
      MRET = 1
      RETURN
C
      ENTRY REFIN (N,MAX,ACC,MRET,NOP)
C     THIS IS A SINGLE ITTERATION REFINEMENT WITHOUT INTERMEDIATE RESULTS.
C     ITS IS CONSIDERABLY MORE EFFICIENT,TIMEWISE, THAN THE GENERAL VERSION.
  716 DO 711 I=1,N
      READ(4) B
      DO 712 II=1,N
      READ (3) A
      C(II)=0.DO
      DO 713 I2=1,N
  713 C(II)=C(II)+A(I2)*B(I2)
  712 CONTINUE
      REWIND 3
      WRITE(2) C
  711 CONTINUE
      REWIND 2
      REWIND 3
```

```
      REWIND 4
      DO 721 I=1,N
      READ(4) B
      DO 722 I1=1,N
      D(I1)=C.CO
      READ(2) A
      DO 723  I2=1,N
  723 D(I1)=C(I1)+A(I2)*B(I2)
  722 CONTINUE
      REWIND 2
      WRITE(1) D
  721 CONTINUE
C
      REWIND 1
      REWIND 2
      REWIND 4
      DO 730 I=1,N
      READ (4) A
      READ(1) B
      DO 731 I1=1,N
  731 D(I1)=A(I1)+A(I1)-B(I1)
      WRITE(2) C
  730 CONTINUE
      REWIND 1
      REWIND 2
      REWIND 4
      DO 735 I=1,N
      READ (2) C
  735 WRITE(4) C
      REWIND 2
      REWIND 4
      MRET=5
      RETURN
  100 FORMAT (1H1,//,1X,'THE REFINED INVERSE MATRIX:ITTERATION NUMBER',
     113,/,1X,47(1H*),///)
  101 FORMAT (//,5X,'ROW NUMBER',I4,/,5X,'--------------',/)
  102 FORMAT (1X,5D25.16 )
  103 FORMAT (1H1,//,1X,'EXECUTION TERMINATING: REFINEMENT NOT POSSIBLE,
     1TRY A NEW FIRST GUESS',/,1X,73(1H-))
  104 FORMAT (1H1,//,1X,'FAILED TO REACH DESIRED ACCURACY IN SPECIFIED I
     1TTERATIONS.',1X,57(1H-),//,5X,'ITTERATIONS SPECIFIED =',I3,/,5X,'C
     2OMPUTED ACCURACY =',G12.3,/,5X,'SPECIFIED ACCURACY =', G12.3,//  )
  105 FORMAT (//,5X,'REPEAT MODE INVOKED:ITTERATION COUNTER RESET TO ZER
     10.'  )
  106 FORMAT (//,5X,'CONVERGENCE TOO SLOW:RE-EXAMIN SITUATION',/,5X'EXEC
     1UTION TERMINATING.')
  107 FORMAT( //,5X,'SATISFACTORY CONVERGENCE OBTAINED:',   /,5X,34(1H*)
     1,//,5X,'NUMBER OF ITTERATIONS MADE ',I2,/,5X,'ATTAINED ACCURACY WA
     2S ', G12.3    )
      END
```

```
C
C     A NON DESTRUCTIVE INVERSE SUBROUTINE ESPECIALLY SUITED TO POSTIVE
C     DEFINITE MATRICES. MAXIMUM SIZE OF THIS VERSION IS 100.
C
      IMPLICIT REAL *8 (A-H,O-Z)
      DIMENSION  A(I,M),B(I,M),P(100)
      N=I-1
      MI=M-1
      DO 1 J=1,I
      DO 1 K=1,I
    1 B(J,K) =A(J,K)
      DO 5 K= 1,I
      DO 2 J= 1,MI
    2 P(J) = B(1,J+1)/B(1,1)
      P(M) = 1.DO /B(1,1)
      DO 4 L =1,N
      DO 3 J =1,MI
    3 B(L,J) = B(L+1,J+1)- B(L+1,1)*P(J)
    4 B(L,M) =-B(L+1, 1 )*P(M)
      DO 5 J =1,M
    5 B(I,J) = P(J)
      RETURN
      END
```

APPENDIX F

ANALYTICAL FORMATION OF THE B MATRIX

(a) Introduction

The most difficult task in photogrammetric adjustments is the formation of the B matrix, more correctly termed the partial matrix of the functions with respect to the unknown parameters.

i.e. $B = \frac{\partial \text{function}}{\partial \text{parameter}}$

The mathematical functions under consideration, equation set (2.5), are conveniently condensed to the following form:

$$x_p = x_o - f\frac{U}{W} = F_1$$

$$y_p = y_o - f\frac{V}{W} = F_2$$

where $U = N_1(X_p - X_o - V\cdot\Delta t)$

$$V = N_2(X_p - X_o - V\cdot\Delta t)$$

$$W = N_3(X_p - X_o - V\cdot\Delta t)$$

Then $$\frac{\partial F_1}{\partial \text{parameter}} = -f\left[W\frac{\partial U}{\partial \text{parameter}} - U\frac{\partial W}{\partial \text{parameter}}\right]\cdot W^{-2}$$

$$\frac{\partial F_2}{\partial \text{parameter}} = -f\left[W\frac{\partial V}{\partial \text{parameter}} - V\frac{\partial W}{\partial \text{parameter}}\right]\cdot W^{-2}$$

for those cases where x_o, y_o, and f can be considered known.

Thus, the problem reduces to the formation of

$$\frac{\partial F_1}{\partial \text{parameter}} \quad \text{and} \quad \frac{\partial F_2}{\partial \text{parameter}}$$

where the parameters are:

camera attitudes: κ, ϕ, ω

attitude rate change: $\dot{\kappa}$, $\dot{\phi}$, $\dot{\omega}$

photostation: X_o, Y_o, Z_o

and photostation velocities: V_x, V_y, V_z

(b) <u>The Partials for the Translational and Linear Velocity Components of the Photostation</u>

Differentiation of $U = N_1(X_p - X_o - V\Delta t)$ yields:

$$\frac{\partial U}{\partial X_o} = N_1 \begin{bmatrix} -1 \\ 0 \\ 0 \end{bmatrix} = -n_{11} \qquad \frac{\partial U}{\partial V_x} = N_1 \begin{bmatrix} -1 \\ 0 \\ 0 \end{bmatrix} \Delta t = -\Delta t \cdot n_{11}$$

$$\frac{\partial U}{\partial Y_o} = N_1 \begin{bmatrix} 0 \\ -1 \\ 0 \end{bmatrix} = -n_{12} \qquad \frac{\partial U}{\partial V_y} = N_1 \begin{bmatrix} 0 \\ -1 \\ 0 \end{bmatrix} \Delta t = -\Delta t \cdot n_{12}$$

$$\frac{\partial U}{\partial Z_o} = N_1 \begin{bmatrix} 0 \\ 0 \\ -1 \end{bmatrix} = -n_{13} \qquad \frac{\partial U}{\partial V_z} = N_1 \begin{bmatrix} 0 \\ 0 \\ -1 \end{bmatrix} \Delta t = -\Delta t \cdot n_{13}$$

Differentiation of $V = N_2(X_p - X_o - V\Delta t)$ yields

$$\frac{\partial V}{\partial X_o} = N_2\begin{bmatrix}-1\\0\\0\end{bmatrix} = -n_{21} \qquad \frac{\partial V}{\partial V_x} = N_2\begin{bmatrix}-1\\0\\0\end{bmatrix}\Delta t = -\Delta t \cdot n_{21}$$

$$\frac{\partial V}{\partial Y_o} = N_2\begin{bmatrix}0\\-1\\0\end{bmatrix} = -n_{22} \qquad \frac{\partial V}{\partial V_y} = N_2\begin{bmatrix}0\\-1\\0\end{bmatrix}\Delta t = -\Delta t \cdot n_{22}$$

$$\frac{\partial V}{\partial Z_o} = N_2\begin{bmatrix}0\\-1\\0\end{bmatrix} = -n_{23} \qquad \frac{\partial V}{\partial V_z} = N_2\begin{bmatrix}0\\0\\-1\end{bmatrix}\Delta t = -\Delta t \cdot n_{23}$$

Differentiation of $W = N_3(X_p - X_o - V \cdot \Delta t)$ yields

$$\frac{\partial W}{\partial X_o} = N_3\begin{bmatrix}-1\\0\\0\end{bmatrix} = -n_{31} \qquad \frac{\partial W}{\partial V_x} = N_3\begin{bmatrix}-1\\0\\0\end{bmatrix}\Delta t = -\Delta t \cdot n_{31}$$

$$\frac{\partial W}{\partial Y_o} = N_3\begin{bmatrix}0\\-1\\0\end{bmatrix} = -n_{32} \qquad \frac{\partial W}{\partial V_y} = N_3\begin{bmatrix}0\\-1\\0\end{bmatrix}\Delta t = -\Delta t \cdot n_{32}$$

$$\frac{\partial W}{\partial Z_o} = N_3\begin{bmatrix}0\\0\\-1\end{bmatrix} = -n_{33} \qquad \frac{\partial W}{\partial V_z} = N_3\begin{bmatrix}0\\0\\-1\end{bmatrix}\Delta t = -\Delta t \cdot n_{33}$$

Then, following the rules of differentiation established at the beginning of this appendix,

$$\frac{\partial F_1}{\partial X_o} = \frac{-f}{W}\left(-n_{11} + n_{31}\frac{U}{W}\right) \qquad \frac{\partial F_2}{\partial X_o} = \frac{-f}{W}\left(-n_{21} + n_{31}\frac{V}{W}\right)$$

$$\frac{\partial F_1}{\partial Y_o} = \frac{-f}{W}\left(-n_{12} + n_{32}\frac{U}{W}\right) \qquad \frac{\partial F_2}{\partial Y_o} = \frac{-f}{W}\left(-n_{22} + n_{32}\frac{V}{W}\right)$$

$$\frac{\partial F_1}{\partial Z_o} = \frac{-f}{W}\left(-n_{13} + n_{33}\frac{U}{W}\right) \qquad \frac{\partial F_2}{\partial Z_o} = \frac{-f}{W}\left(-n_{23} + n_{33}\frac{V}{W}\right)$$

$$\frac{\partial F_1}{\partial V_x} = \frac{-\Delta t \cdot f}{W}\left(-n_{11} + n_{31}\frac{U}{W}\right) \qquad \frac{\partial F_2}{\partial V_x} = \frac{-\Delta t \cdot f}{W}\left(-n_{21} + n_{31}\frac{V}{W}\right)$$

$$= \Delta t \cdot \frac{\partial F_1}{\partial X_o} \qquad = \Delta t \cdot \frac{\partial F_2}{\partial X_o}$$

$$\frac{\partial F_1}{\partial V_y} = \frac{-\Delta t \cdot f}{W}\left(-n_{12} + n_{32}\frac{U}{W}\right) \qquad \frac{\partial F_2}{\partial V_y} = \frac{-\Delta t \cdot f}{W}\left(-n_{22} + n_{32}\frac{V}{W}\right)$$

$$= \Delta t \cdot \frac{\partial F_1}{\partial Y_o} \qquad = \Delta t \cdot \frac{\partial F_2}{\partial Y_o}$$

$$\frac{\partial F_1}{\partial V_z} = \frac{-\Delta t \cdot f}{W}\left(-n_{13} + n_{33}\frac{U}{W}\right) \qquad \frac{\partial F_2}{\partial V_z} = \frac{-\Delta t \cdot f}{W}\left(-n_{23} + n_{33}\frac{V}{W}\right)$$

$$= \Delta t \cdot \frac{\partial F_1}{\partial Z_o} \qquad = \Delta t \cdot \frac{\partial F_2}{\partial Y_o}$$

(c) <u>The Partials for the Attitude and Attitude Velocity Components of the Photostation</u>

The derivation of the rotation terms is analogous to that of the translational and linear velocity components.

It is again convenient to use the compressed notation of Section (a) of this appendix. That is,

$$\begin{bmatrix} U \\ V \\ W \end{bmatrix} = N(X_p - X_o - V\Delta t)$$

$$= R_\kappa R_{\dot\kappa \Delta t} R_\phi R_{\dot\phi \Delta t} R_\omega R_{\dot\omega \Delta t}(X_p - X_o - V\Delta t)$$

$$\text{Hence} \quad \begin{bmatrix} \frac{\partial U}{\partial \kappa} \\ \frac{\partial V}{\partial \kappa} \\ \frac{\partial W}{\partial \kappa} \end{bmatrix} = \frac{\partial N}{\partial \kappa} (X_p - X_o - V\Delta t)$$

It is also necessary, therefore, to form similar expressions for:

$$\frac{\partial N}{\partial \phi}, \quad \frac{\partial N}{\partial \omega}, \quad \frac{\partial N}{\partial \dot{\kappa}}, \quad \frac{\partial N}{\partial \dot{\phi}}, \quad \frac{\partial N}{\partial \dot{\omega}}$$

This can be greatly simplified by using skew symmetric matrices.

The differentiation is as follows:

$$\frac{\partial N}{\partial \kappa} = \frac{\partial R_\kappa}{\partial \kappa} \cdot R_{\dot{\kappa}\Delta t} \cdot R_\phi \cdot R_{\dot{\phi}\Delta t} \cdot R_\omega \cdot R_{\dot{\omega}\Delta t} = P_3 N$$

$$\frac{\partial N}{\partial \dot{\kappa}} = R_\kappa \cdot \frac{\partial R_{\dot{\kappa}\Delta t}}{\partial \dot{\kappa}} \cdot R_\phi \cdot R_{\dot{\phi}\Delta t} \cdot R_\omega \cdot R_{\dot{\omega}\Delta t}$$

$$= \Delta t \cdot R_\kappa \cdot P_3 \cdot R_{\dot{\kappa}\Delta t} \cdot R_\phi \cdot R_{\dot{\phi}\Delta t} \cdot R_\omega \cdot R_{\dot{\omega}\Delta t}$$

$$= \Delta t \cdot R_\kappa \cdot P_3 \cdot R_\kappa^T \cdot R_\kappa \cdot R_{\dot{\kappa}\Delta t} \cdot R_\phi \cdot R_{\dot{\phi}\Delta t} \cdot R_\omega \cdot R_{\dot{\omega}\Delta t}$$

$$= \Delta t \cdot Q_1 \cdot N \quad \text{where} \quad Q_1 = R_\kappa \cdot P_3 \cdot R_\kappa^T$$

$$\frac{\partial N}{\partial \phi} = R_\kappa \cdot R_{\dot{\kappa}\Delta t} \cdot \frac{\partial R_\phi}{\partial \phi} \cdot R_{\dot{\phi}\Delta t} \cdot R_\omega \cdot R_{\dot{\omega}\Delta t}$$

$$= R_\kappa \cdot R_{\dot{\kappa}\Delta t} \cdot P_2 \cdot R_\phi \cdot R_{\dot{\phi}\Delta t} \cdot R_\omega \cdot R_{\dot{\omega}\Delta t}$$

$$= R_\kappa \cdot R_{\dot{\kappa}\Delta t} \cdot P_2 \cdot R_{\dot{\kappa}\Delta t}^T \cdot R_\kappa^T \cdot R_\kappa \cdot R_{\dot{\kappa}\Delta t} \cdot R_\phi \cdot R_{\dot{\phi}\Delta t} \cdot R_\omega \cdot R_{\dot{\omega}\Delta t}$$

$$= Q_2 \cdot N \quad \text{where} \quad Q_2 = R_\kappa \cdot R_{\dot{\kappa}\Delta t} \cdot P_2 \cdot R_{\dot{\kappa}\Delta t}^T \cdot R_\kappa^T$$

$$\frac{\partial N}{\partial \dot{\phi}} = R_{\kappa} \cdot R_{\dot{\kappa}\Delta t} \cdot R_{\phi} \cdot \frac{\partial R_{\dot{\phi}\Delta t}}{\partial \dot{\phi}} \cdot R_{\omega} \cdot R_{\dot{\omega}\Delta t}$$

$$= \Delta t \cdot R_{\kappa} \cdot R_{\dot{\kappa}\Delta t} \cdot R_{\phi} \cdot R_{\dot{\phi}\Delta t} \cdot P_2 \cdot R_{\omega} \cdot R_{\dot{\omega}\Delta t}$$

$$= \Delta t \cdot R_{\kappa} \cdot R_{\dot{\kappa}\Delta t} \cdot R_{\phi} \cdot R_{\dot{\phi}\Delta t} \cdot R_{\omega} \cdot R_{\dot{\omega}\Delta t} \cdot R^{T}_{\dot{\omega}\Delta t} \cdot R^{T}_{\omega} \cdot P_2 \cdot R_{\omega} \cdot R_{\dot{\omega}\Delta t}$$

$$= t \cdot N \cdot Q_3 \quad \text{where} \quad Q_3 = R^{T}_{\dot{\omega}\Delta t} \cdot R^{T}_{\omega} \cdot P_2 \cdot R_{\omega} \cdot R_{\dot{\omega}\Delta t}$$

$$\frac{\partial N}{\partial \omega} = R_{\kappa} \cdot R_{\dot{\kappa}\Delta t} \cdot R_{\phi} \cdot R_{\dot{\phi}\Delta t} \cdot \frac{\partial R_{\omega}}{\partial \omega} \cdot R_{\dot{\omega}\Delta t}$$

$$= R_{\kappa} \cdot R_{\dot{\kappa}\Delta t} \cdot R_{\phi} \cdot R_{\dot{\phi}\Delta t} \cdot R_{\omega} \cdot P_1 \cdot R_{\dot{\omega}\Delta t}$$

$$= R_{\kappa} \cdot R_{\dot{\kappa}\Delta t} \cdot R_{\phi} \cdot R_{\dot{\phi}\Delta t} \cdot R_{\omega} \cdot R_{\dot{\omega}\Delta t} \cdot R^{T}_{\dot{\omega}\Delta t} \cdot P_1 \cdot R_{\dot{\omega}\Delta t}$$

$$= N \cdot Q_4 \quad \text{where} \quad Q_4 = R^{T}_{\dot{\omega}\Delta t} \cdot P_1 \cdot R_{\dot{\omega}\Delta t}$$

$$\frac{\partial N}{\partial \dot{\omega}} = R_{\kappa} \cdot R_{\dot{\kappa}\Delta t} \cdot R_{\phi} \cdot R_{\dot{\phi}\Delta t} \cdot R_{\omega} \cdot \frac{\partial R_{\dot{\omega}\Delta t}}{\partial \dot{\omega}} = \Delta t \cdot N \cdot P_1$$

Hence the partials of U, V and W with respect to the attitudes and attitude rate changes are:

$$\begin{bmatrix} \frac{\partial U}{\partial \kappa} \\ \frac{\partial V}{\partial \kappa} \\ \frac{\partial W}{\partial \kappa} \end{bmatrix} = P_1 \cdot N \cdot (X_p - X_o - V\Delta t) \qquad \begin{bmatrix} \frac{\partial U}{\partial \dot{\kappa}} \\ \frac{\partial V}{\partial \dot{\kappa}} \\ \frac{\partial W}{\partial \dot{\kappa}} \end{bmatrix} = \Delta t \cdot Q_1 \cdot N \cdot (X_p - X_o - V\Delta t)$$

$$\begin{bmatrix} \frac{\partial U}{\partial \phi} \\ \frac{\partial V}{\partial \phi} \\ \frac{\partial W}{\partial \phi} \end{bmatrix} = Q_2 \cdot N \cdot (X_p - X_o - V\Delta t) \qquad \begin{bmatrix} \frac{\partial U}{\partial \dot{\phi}} \\ \frac{\partial V}{\partial \dot{\phi}} \\ \frac{\partial W}{\partial \dot{\phi}} \end{bmatrix} = \Delta t \cdot N \cdot Q_3' (X_p - X_o - V\Delta t)$$

$$\begin{bmatrix} \frac{\partial U}{\partial \omega} \\ \frac{\partial V}{\partial \omega} \\ \frac{\partial W}{\partial \omega} \end{bmatrix} = N \cdot Q_4 \cdot (X_p - X_o - V\Delta t) \qquad \begin{bmatrix} \frac{\partial U}{\partial \dot{\omega}} \\ \frac{\partial V}{\partial \dot{\omega}} \\ \frac{\partial W}{\partial \dot{\omega}} \end{bmatrix} = \Delta t \cdot N \cdot P_1 (X_p - X_o - V\Delta t)$$

Substitution of these expressions into the following quotient rule formulae will yield the appropriate terms.

$$\frac{\partial F_1}{\partial \kappa} = \frac{-f}{W}\left(\frac{\partial U}{\partial \kappa} - \frac{U}{W}\frac{\partial W}{\partial \kappa}\right) \qquad \frac{\partial F_2}{\partial \kappa} = \frac{-f}{W}\left(\frac{\partial V}{\partial \kappa} - \frac{V}{W}\frac{\partial W}{\partial \kappa}\right)$$

$$\frac{\partial F_1}{\partial \dot{\kappa}} = \frac{-f}{W}\left(\frac{\partial U}{\partial \dot{\kappa}} - \frac{U}{W}\frac{\partial W}{\partial \dot{\kappa}}\right) \qquad \frac{\partial F_2}{\partial \dot{\kappa}} = \frac{-f}{W}\left(\frac{\partial V}{\partial \dot{\kappa}} - \frac{V}{W}\frac{\partial W}{\partial \dot{\kappa}}\right)$$

$$\frac{\partial F_1}{\partial \phi} = \frac{-f}{W}\left(\frac{\partial U}{\partial \phi} - \frac{U}{W}\frac{\partial W}{\partial \phi}\right) \qquad \frac{\partial F_2}{\partial \phi} = \frac{-f}{W}\left(\frac{\partial V}{\partial \phi} - \frac{V}{W}\frac{\partial W}{\partial \phi}\right)$$

$$\frac{\partial F_1}{\partial \dot{\phi}} = \frac{-f}{W}\left(\frac{\partial U}{\partial \dot{\phi}} - \frac{U}{W}\frac{\partial W}{\partial \dot{\phi}}\right) \qquad \frac{\partial F_2}{\partial \dot{\phi}} = \frac{-f}{W}\left(\frac{\partial V}{\partial \dot{\phi}} - \frac{V}{W}\frac{\partial W}{\partial \dot{\phi}}\right)$$

$$\frac{\partial F_1}{\partial \omega} = \frac{-f}{W}\left(\frac{\partial U}{\partial \omega} - \frac{U}{W}\frac{\partial W}{\partial \omega}\right) \qquad \frac{\partial F_2}{\partial \omega} = \frac{-f}{W}\left(\frac{\partial V}{\partial \omega} - \frac{V}{W}\frac{\partial W}{\partial \omega}\right)$$

$$\frac{\partial F_1}{\partial \dot{\omega}} = \frac{-f}{W}\left(\frac{\partial U}{\partial \dot{\omega}} - \frac{U}{W}\frac{\partial W}{\partial \dot{\omega}}\right) \qquad \frac{\partial F_2}{\partial \dot{\omega}} = \frac{-f}{W}\left(\frac{\partial V}{\partial \dot{\omega}} - \frac{V}{W}\frac{\partial W}{\partial \dot{\omega}}\right)$$

(d) Partials Associated with the Survey Data

It is also necessary to form the partials with respect to the ground coordinates for application in the total block situation. The same quotient rules that were used to determine the partials with respect to the unknowns are used here with the same notation.

Differentiation of $U = N_1(X_p - X_o - V\Delta t)$ yields

$$\frac{\partial U}{\partial X_p} = N_1 \begin{bmatrix} 1 \\ 0 \\ 0 \end{bmatrix} = n_{11}$$

$$\frac{\partial U}{\partial Y_p} = N_1 \begin{bmatrix} 0 \\ 1 \\ 0 \end{bmatrix} = n_{12}$$

$$\frac{\partial U}{\partial Z_p} = N_1 \begin{bmatrix} 0 \\ 0 \\ 1 \end{bmatrix} = n_{13}$$

Differentiation of $V = N_2(X_p - X_o - V\Delta t)$ yields

$$\frac{\partial V}{\partial X_p} = N_2 \begin{bmatrix} 1 \\ 0 \\ 0 \end{bmatrix} = n_{21}$$

$$\frac{\partial V}{\partial Y_p} = N_2 \begin{bmatrix} 0 \\ 1 \\ 0 \end{bmatrix} = n_{22}$$

$$\frac{\partial V}{\partial Z_p} = N_2 \begin{bmatrix} 0 \\ 0 \\ 1 \end{bmatrix} = n_{23}$$

Differentiation of $W = N_3(X_p - X_o - V\Delta t)$ yields

$$\frac{\partial W}{\partial X_p} = N_3 \begin{bmatrix} 1 \\ 0 \\ 0 \end{bmatrix} = n_{31}$$

$$\frac{\partial W}{\partial Y_p} = N_3 \begin{bmatrix} 0 \\ 1 \\ 0 \end{bmatrix} = n_{32}$$

$$\frac{\partial W}{\partial Z_p} = N_3 \begin{bmatrix} 0 \\ 0 \\ 1 \end{bmatrix} = n_{33}$$

and hence

$$\frac{\partial F_1}{\partial X_p} = \frac{-f}{W}\left(n_{11} - n_{31}\frac{U}{W}\right) \qquad \frac{\partial F_2}{\partial X_p} = \frac{-f}{W}\left(n_{21} - n_{31}\frac{V}{W}\right)$$

$$= \frac{-\partial F_1}{\partial X_o} \qquad = \frac{-\partial F_2}{\partial X_o}$$

$$\frac{\partial F_1}{\partial Y_p} = \frac{-f}{W}\left(n_{12} - n_{32}\frac{U}{W}\right) \qquad \frac{\partial F_2}{\partial Y_p} = \frac{-f}{W}\left(n_{22} - n_{32}\frac{V}{W}\right)$$

$$= \frac{-\partial F_1}{\partial Y_o} \qquad = \frac{-\partial F_2}{\partial Y_o}$$

$$\frac{\partial F_1}{\partial Z_p} = \frac{-f}{W}\left(n_{13} - n_{33}\frac{U}{W}\right) \qquad \frac{\partial F_2}{\partial Z_p} = \frac{-f}{W}\left(n_{23} - n_{33}\frac{V}{W}\right)$$

$$= \frac{-\partial F_1}{\partial Z_o} \qquad = \frac{-\partial F_2}{\partial Z_o}$$

BIBLIOGRAPHY

1. Army Map Service, USA, and Aeronautical Chart and Information Center, USAF, Department of Defense Selenodetic Control System 1966, Washington, D. C., Department of the Army, Corps of Engineers, Army Map Service, 1967.

2. Rindfleisch, T., "Photometric Method for Lunar Topography," Photogrammetric Engineering, Vol. 32, No. 2, 1966, pp. 262-276.

3. Beeler, M., and Michlovitz, K., Lunar Orbiter Photographic Data, Data Users' Note NSSDC 69-05, Greenbelt, Md., National Aeronautics and Space Administration, Goddard Space Flight Center, 1969.

4. Eastman Kodak Company, Photographic Subsystem Reference Handbook for the Lunar Orbiter Program, (NASA reference number L-018375-Ru), Prepared for The Boeing Company, Space Division, 1966.

5. Konecny, G., "Some Problems in the Evaluation of Lunar Orbiter Photography," The Canadian Surveyor, Vol. 22, No. 4, 1968, pp. 394-412.

6. Kosofsky, L. J., "Topography from Lunar Orbiter Photographs," Photogrammetric Engineering, Vol. 32, No. 2, 1966, pp. 277-285.

7. Norman, P. E., "Out of this World Photogrammetry," Photogrammetric Engineering, Vol. 35, No. 7, 1969, pp. 693-701.

8. United States Air Force, Aeronautical Chart and Information Center, Lunar-Planetary Branch, Cartography Division, Lunar Orbiters IV and V: Camera Calibration Report, St. Louis, Missouri, 1968.

9. Brown, Duane C., Calibration of Three High Resolution Lunar Orbiter Cameras, Final Report Prepared for The Boeing Company, Space Division, Melbourne, Florida, D. Brown Associates, Inc., 1967.

10. Wong, K. W., "Geometric Distortions in Television Imageries," Photogrammetric Engineering, Vol. 35, No. 5, 1969, pp. 493-500.

11. Wolfe, R. N., and Lamberts, R. L., "The Effect of Image Motion on Resolving Power," Photographic Engineering, Vol. 6, No. 4, 1955, pp. 270-274.

12. Trott, T., "The Effects of Motion on Resolution," Photogrammetric Engineering, Vol. 26, No. 5, 1960, pp. 819-827.

13. Rosenau, M. D., "Parabolic Image-Motion," Photogrammetric Engineering, Vol. 27, No. 3, 1961, pp. 421-427.

14. Kawachi, D. A., and Weinflash, D., Image Motion in Aerial Photographs Resulting from Vehicle Rotations, Fairchild Space and Defense Systems Technical Memo No. SME-AV-1, Fairchild Camera and Instrument Corporation, 1963.

15. Kawachi, D. A., "Image Motion Due to Camera Rotation," Photogrammetric Engineering, Vol. 31, No. 5, 1965, pp. 861-867.

16. Kawachi, D. A., "Image Motion and Its Compensation for the Oblique Frame Camera," Photogrammetric Engineering, Vol. 31, No. 1, 1965, pp. 154-164.

17. American Society of Photogrammetry, Manual of Photogrammetry, 3rd edition, Falls Church, Virginia, 1966.

18. Faddeev, D. K., and Faddeeva, V. N., Computational Methods of Linear Algebra, San Francisco, Freeman, 1963.

19. International Business Machines, System/360 Scientific Subroutine Package (360A-CM-03X) Version III - Programmers Manual, IBM Manual No. H20-0205-3, White Plain, N. Y., IBM Technical Publications Branch, 1968.

20. Brown, Duane C., Trotter, J. E., SAGA, A Computer Program for Short Arc Geodetic Adjustment of Satellite Observations, Final Report, Contract Number F19628-68-C-0093, For Air Force Cambridge Research Laboratories, Bedford, Massachusetts, Office of Aerospace Research, United States Air Force, 1969.

21. Brown, Duane, C., "Inversion of Very Large Matrices Encountered in Large Scale Problems of Photogrammetry and Photographic Astrometry," Proceedings, Conference on Photographic Astrometric Technique, University of South Florida, Tampa, March, 1968.

22. Snowden, J. M., An Investigation of Practical Solutions of Large Systems of Normal Equations, M. Sc. Thesis, The Ohio State University, 1966.

23. Elassal, A. A., "Algorithm for the General Analytical Solution," Photogrammetric Engineering, Vol. 35, No. 12, 1969, pp. 1268-1277.

24. Uotila, U. A., Introduction to Adjustment Computations with Matrices, Unpublished lecture notes, Department of Geodetic Science, The Ohio State University, 1967.

25. Berezin, I. S., and Zhidkov, N. P., Computing Methods, Vol. 2, Oxford, Pergamon Press, 1965.

26. Needham, P., The Formation and Evaluation of Detailed Geopotential Models Based on Point Masses, Ph. D. Dissertation, The Ohio State University, 1970.

27. Albasiny, E. L., "Error in Digital Solution of Linear Problems," in "Error in Digital Computation, Vol. 1," Proceedings of an Advanced Seminar Conducted by the Mathematics Research Center, U. S. Army at the University of Wisconsin, Madison, October 1964, New York, J. Wiley, 1965.

28. Turing, A. M., "Rounding off Errors in Matrix Processes," Quarterly Journal of Mechanics and Applied Mathematics, Vol. 1, 1948, pp. 287-308.

29. Todd, J., "The Condition of Certain Matrices I," Quarterly Journal of Mechanics and Applied Mathematics, Vol. 2, 1949, pp. 469-472.

30. Newman, M., and Todd, J., "The Evaluation of Matrix Inversion Programs," Journal SIAM, Vol. 6, 1958, pp. 466-476.

31. Savage, R., and Lukacs, E., "Tables of Inverses of Finite Segments of the Hilbert Matrix," in Contributions to the Solution of Systems of Linear Equations and the Determination of Eigenvalues, National Bureau of Standards, Applied Mathematics Series, No. 39, 1954, pp. 105-108.

32. Todd, J., "The Condition of a Finite Segment of the Hilbert Matrix," in Contributions to the Solution of Systems of Linear Equations and the Determination of Eigenvalues, National Bureau of Standards, Applied Mathematics Series, No. 39, 1954, pp. 109-116.

33. Meissl, P., "Über zufällige Fehler in regelmäßigen gestreckten Ketten," Zeitschrift für Vermessungswesen, Vol. 94, Jah. 1969, Heft 1, pp. 14-26.

34. Gregory, R. T., and Karney, D. L., A Collection of Matrices for Testing Computational Algorithms, New York, Wiley-Interscience, 1969.

35. Wilkinson, J. H., The Algebraic Eigenvalue Problem, Oxford, Clarendon Press, 1965.

36. Hotelling, H., "Analysis of a Complex of Statistical Variables into Principal Components," Journal of Educational Psychology, Vol. 24, Nos. 6 and 7, 1933, pp. 417-441 and 498-520.

37. Dwyer, P. S., and Waugh, F. V., "On Errors in Matrix Inversion," Journal of American Statistical Association, Vol. 48, No. 262, 1953, pp. 289-319.

38. Householder, A. S., in Editor's Preface to Monte Carlo Method, National Bureau of Standards, Applied Mathematics Series, No. 12, 1951.

39. Oswald, F. J., "Matrix Inversion by Monte Carlo Methods," in Mathematical Methods for Digital Computers edited by A. Ralston and H. Will, New York, J. Wiley, 1960.

40. Richardus, P., Project Surveying, Amsterdam, North-Holland Publishing Co., 1966.

41. Brown, Duane C., Results in Geodetic Photogrammetry 1, The Precise Determination of the Location of Bermuda from Photogrammetric Observations of Flares Ejected from Juno 11, RCA Report No. 54.

42. Johnson, F. C., Brown, D. C., Davis, R. G., Research in Mathematical Targeting: The Practical and Rigorous Adjustment of Large Photogrammetric Nets, Report prepared for Rome Air Development Centre, Griffiths Air Force Base, N. Y., under contract AF 30(602)-3007, 1964.

43. Uotila, U., Private Communication, July 1970.

44. Das, G. B., Research Notes on Aerotriangulation, Report No. 142, Department of Geodetic Science, The Ohio State University, 1970.

45. National Mapping Council of Australia, Standard Definitions of Terms Used in Photogrammetric Surveying and Mapping, Prepared on Behalf of the National Mapping Council of Australia by The Director of National Mapping, Department of National Development, Canberra, A. C. T., Australia, 1963.

46. Lucas, J. R., "Differentiation of the Orientation Matrix by Matrix Multipliers," Photogrammetric Engineering, Vol. 29, No. 4, 1963, pp. 708-715.